UNIVERSITY OF LIVERPOOL

Dalla giunzione pn al rivelatore a semiconduttore

G. Casse

Scuola Nazionale "Rivelatori ed Elettronica per Fisica delle Alte Energie, Astrofisica, Applicazioni Spaziali e Fisica Medica"
INFN Laboratori Nazionali di Legnaro, 11-15 Aprile 2011

OUTLINE

- Reminder of radiation-matter interaction
- Semiconductor material properties
- p-n junctions
- Using a p-n junction as a ionising radiation detector
- Advantages of semiconductor (silicon) detectors
- Segmenting detectors for high resolution on hit position
- Main properties of segmented position detectors
- Quick review of various geometries
- Example of (very) complex tracking systems

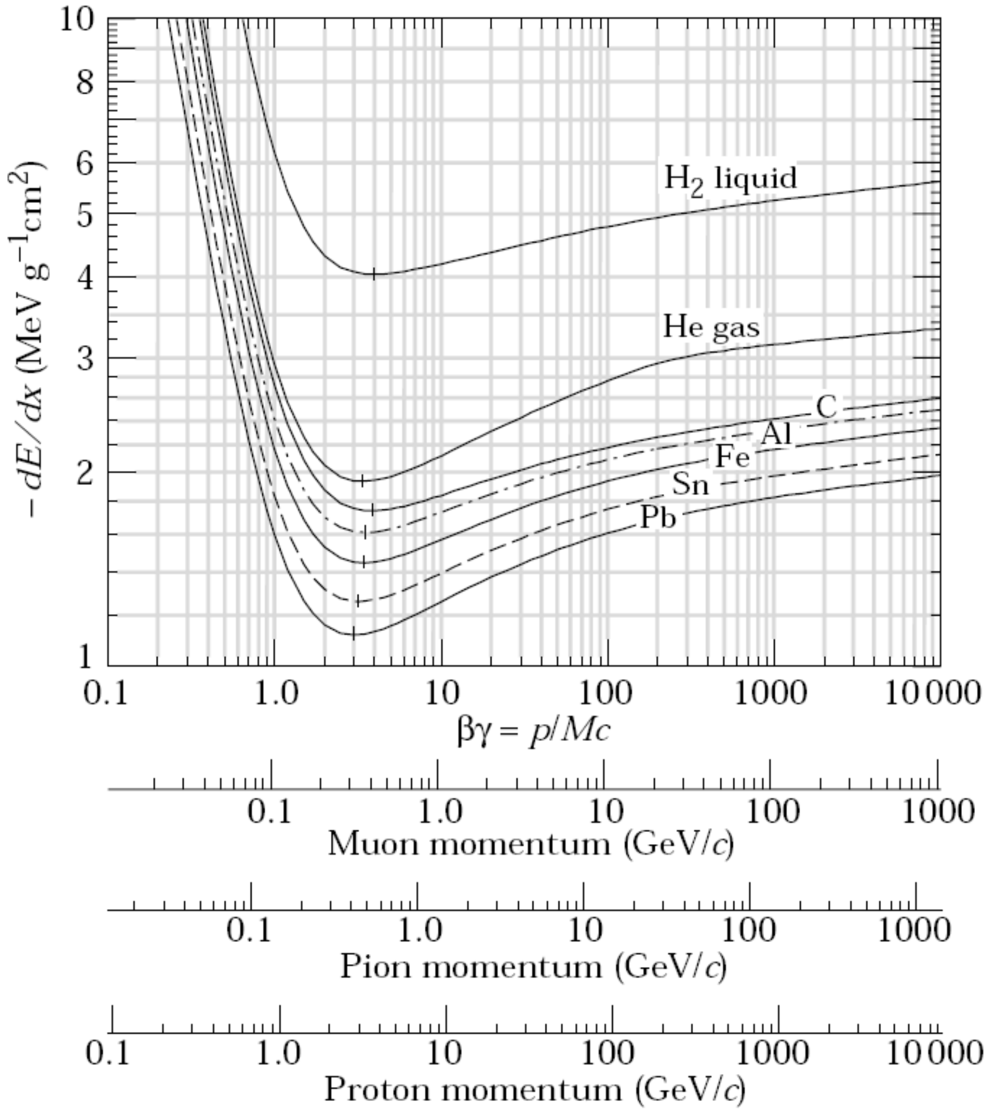

Charged particles

dE/dx vs E for protons in silicon.

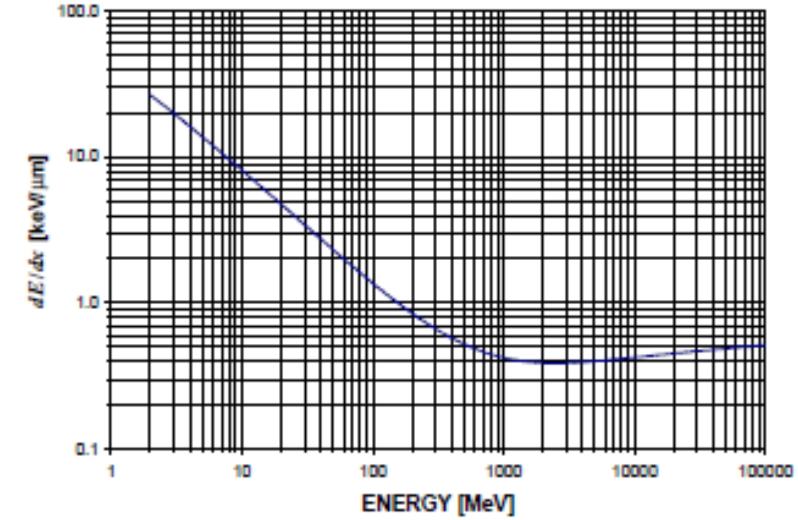

$$\frac{\overline{\Delta E}}{\Delta x} = 2C\frac{m_e c^2}{\beta^2}\frac{Zz^2}{A}\rho\left[\frac{1}{2}\ln\left(\frac{2\gamma^2\beta^2 m_e c^2 E_{\max}}{I_0^2}\right) - \beta^2 - \frac{\varepsilon}{2} - \frac{\delta(\beta)}{2}\right]$$

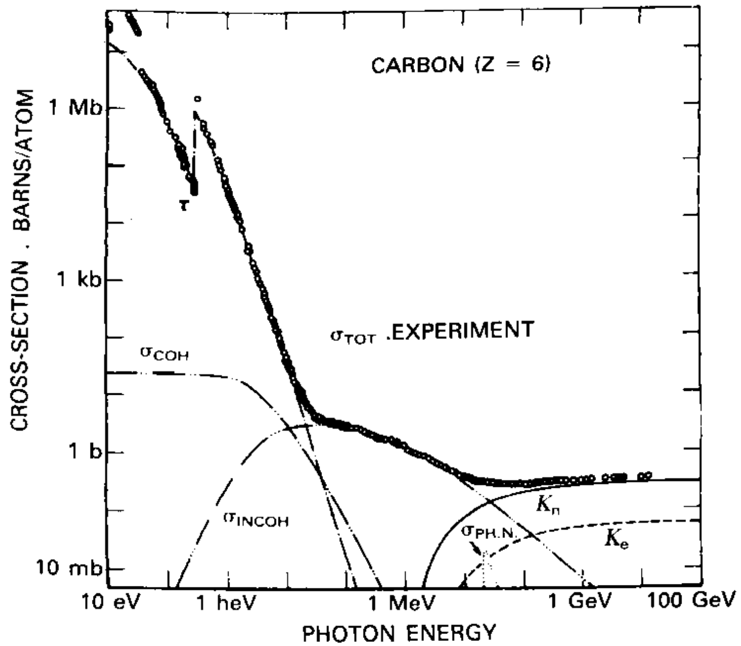

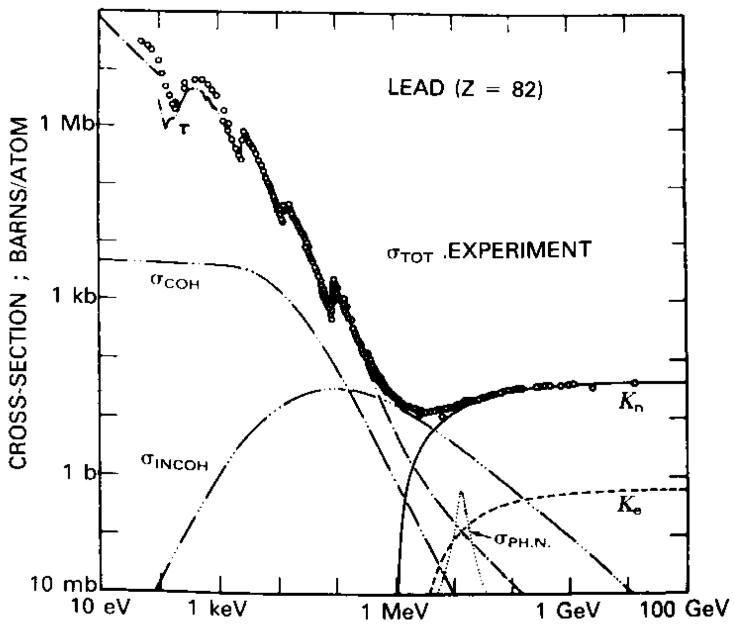

Photons

Photoelectric effect
Compton scattering
Pair production

What you want – what you get

Generally, we want to measure one or more of the following:

- 1. **Energy of particle**, or its dE/dx
- 2. **Momentum of particle** ($\Rightarrow$ position if in a magnetic field)
- 3. **Time of particle's passage** ($\Rightarrow$ position by TOF, or…)
- 4. **Number of particles**, or number of particles per unit area

What we end up measuring is:

- 1. **Charge** [assume $q \propto E$]
- 2. **Charge** [q(x,y) determines position]
- 3. **Charge** $\rightarrow V \rightarrow V(t) > V_T$ at time t
- 4. **Charge** [assume $q(x,y) \propto N(x,y)$]

Particle interaction in sensing/detecting medium creates charge/light/heat …

Material properties - semiconductors

Silicon, germanium und diamond are group IV elements. The crystal structure is the diamond lattice, consisting of 2 interpenetrating sublattices shifted by one quarter along the diagonal of the cube. Each atom is surrounded by four equidistant neighbours.

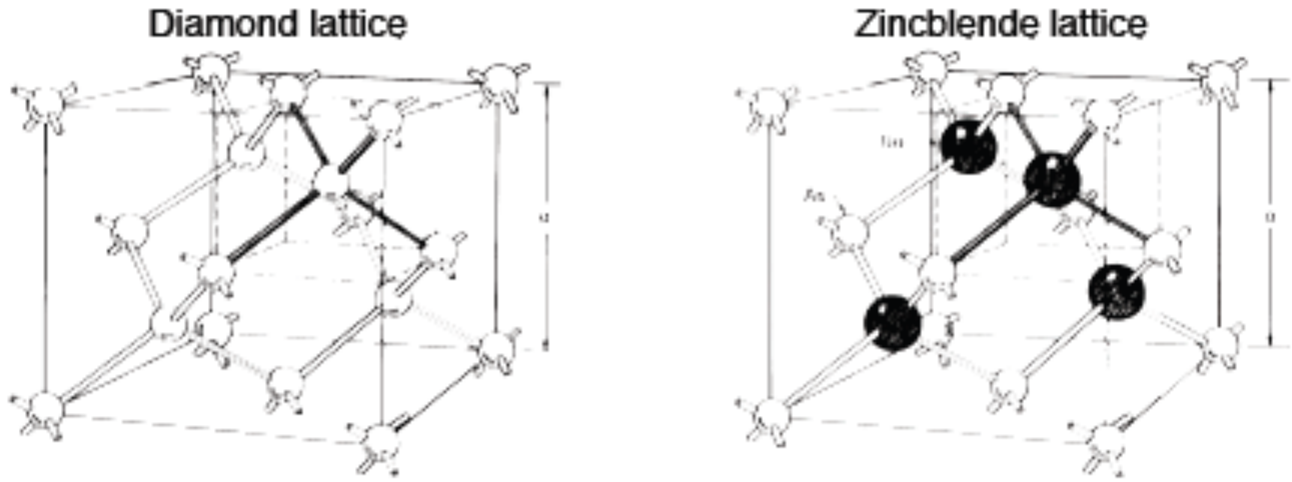

Most III-V semiconductors (e.g. GaAs) have a zincblende lattice. This lattice is similar to the diamond lattice, except that each sublattice consists of one element.

Bond model of semiconductors

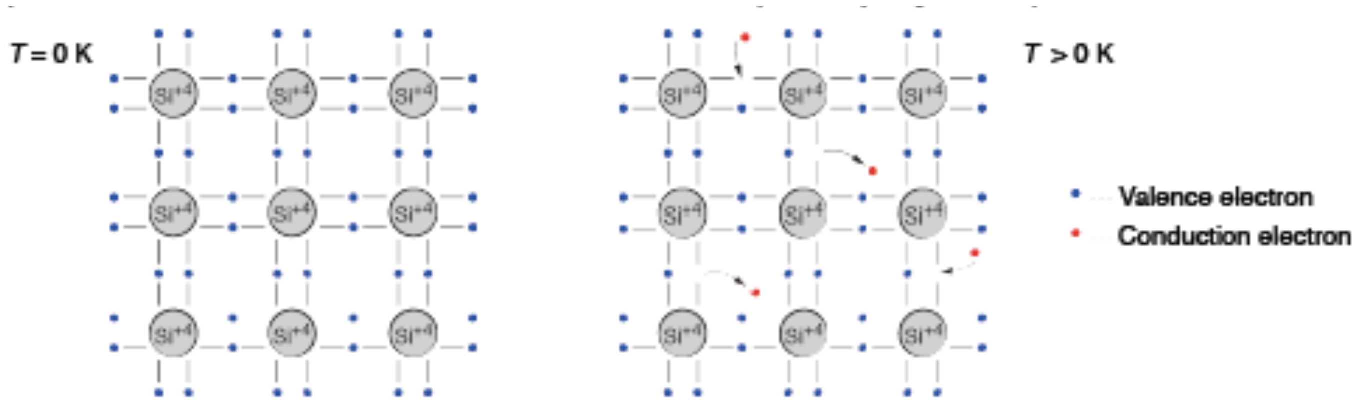

2D projection of the crystal structure.

- Each atom has 4 closest neighbours, the 4 electrons in the outer shell are shared and form covalent bonds.

At low temperature all electrons are bound

At higher temperature thermal vibrations break some of the bonds ➔ free e^- cause conductivity (electron conduction)

The remaining open bonds attract other e^- ➔ The "holes" change position (h conduction)

Energy bands in semiconductors, conductors and isolators

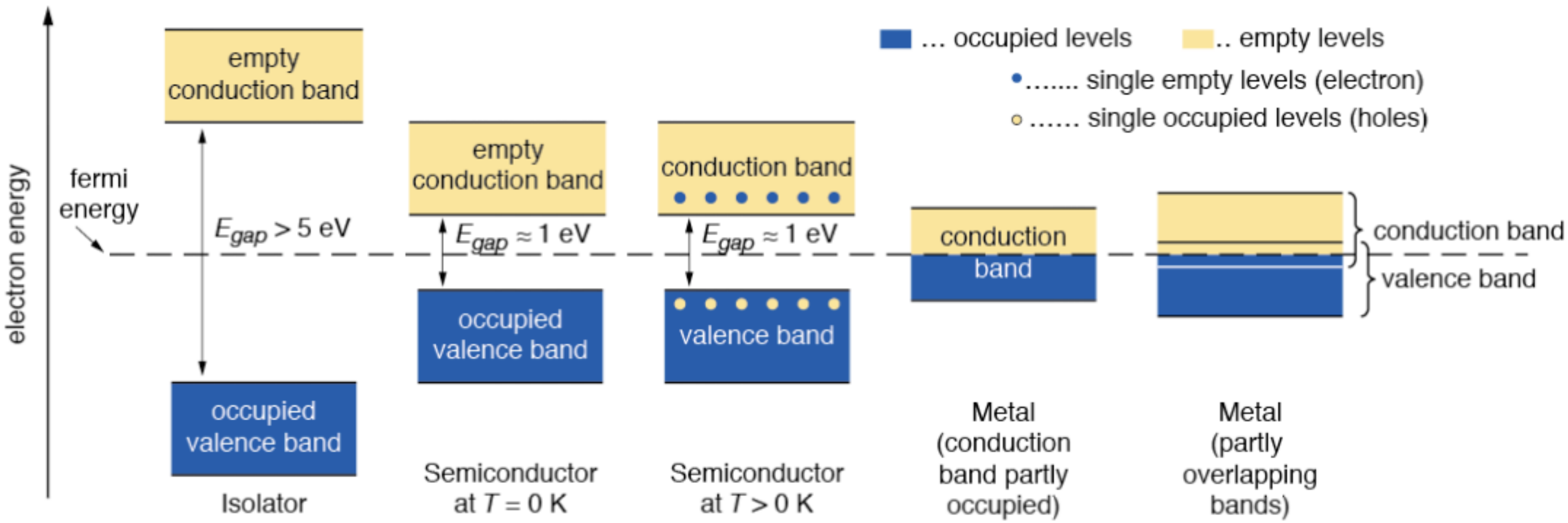

In an isolated atom the electrons have only discrete energy levels. In a solid state material the atomic levels merge to energy bands. In metals the conduction and the valence band overlap, whereas in isolators and semiconductors these levels are separated by an energy gap (band gap). In isolators this gap is large.
Fermi distribution f(*E) describes the probability that an electronic state with* energy E is occupied by an electron.

$$f(E) = \frac{1}{1 + e^{\frac{E - E_F}{kT}}}$$

Charge carrier concentration in semiconductors

Due to the small band gap in semiconductors electrons already occupy the conduction band at room temperature.
Electrons from the conduction band may recombine with holes. A thermal equilibrium is reached between excitation and recombination:
Charge carrier concentration
$n_e = n_h = n_i$
This is called intrinsic carrier concentration:

$$n_i = \sqrt{N_C N_V} \cdot \exp\left(-\frac{E_g}{2kT}\right) \propto T^{\frac{3}{2}} \cdot \exp\left(-\frac{E_g}{2kT}\right)$$

In pure silicon the intrinsic carrier concentration is **$1.45 \cdot 10^{10}$ cm^{-3}**.
With approximately 10^{22} Atoms/cm^3 about 1 in 10^{12} silicon atoms is ionised.

Drift velocity
For electrons:

$$\vec{v}_n = -\mu_n \cdot \vec{E}$$

Drift velocity
For holes:

$$\vec{v}_p = \mu_p \cdot \vec{E}$$

Mobility
For electrons:

$$\mu_n = e\tau_n/m_n$$

Mobility
For electrons:

$$\mu_p = e\tau_p/m_p$$

$\tau_{n,p}$ mean free time between collisions; $\mathbf{m}_{n,p}$ effective mass (e,h); **E** electric field.

Resistivity

$$\rho = \frac{1}{e(\mu_n n_e + \mu_p n_h)}$$

In silicon the mobilities are in good approximation constant below an electric field of ≈ 1 kV/cm.

At $T = 300\ K$:

$\mu_n(Si,\ 300\ K) \approx 1450\ cm^2/Vs$

$\mu_p(Si,\ 300\ K) \approx 450\ cm^2/Vs$

The charge carrier concentration in pure silicon (i.e. intrinsic Si) for T = 300 K is:

$n_e = n_h \approx 1.45 \cdot 10^{10}\ cm^{-3}$

This yields an intrinsic resistivity of:

$\rho \approx 230\ k\Omega cm$

Material	Si	Ge	GaAs	GaP	CdTe	Diamond*
Atomic number Z	14	32	31+33	31+15	48+52	6
Atomgewicht A (amu)	28.086	72.61	69.72+74.92	69.72+30.97	112.4+127.6	12.011
Lattice constant a (Å)	5.431	5.646	5.653	5.451	6.482	3.567
Density ρ (g/cm^3)	2.328	5.326	5.32	4.13	5.86	3.52
E_g (eV) bei 300 K	1.11	0.66	1.42	2.26	1.44	5.47–5.6
E_g (eV) bei 0 K	1.17	0.74	1.52	2.34	1.56	≈ 6
rel. permittivity $\varepsilon_r = \varepsilon / \varepsilon_0$	11.9	16.0	12.8	11.1	10.9	5.7
Melting point (°C)	1415	938	1237	1477	1040	3527
eff. e^--mass (m_n/m_e)	0.98, 0.19	1.64, 0.08	0.067	0.82	0.11	0.2
eff. hole mass$^+$ (m_h/m_e)	0.16	0.044	0.082	0.14	0.35	0.25
eff. density of states in conduction band n_{CB} (cm^{-3})	$3 \cdot 10^{19}$	$1 \cdot 10^{19}$	$4.7 \cdot 10^{17}$	$2 \cdot 10^{19}$		$\approx 10^{20}$
eff. Density of states in valence band n_{VB} (cm^{-3})	$1 \cdot 10^{19}$	$6 \cdot 10^{18}$	$7 \cdot 10^{18}$	$2 \cdot 10^{19}$		$\approx 10^{19}$
Electron mobility μ_e bei 300 K (cm^2/Vs)	~1450	3900	8500	< 300	1050	1800
Hole mobility μ_h bei 300 K (cm^2/Vs)	~450	1900	400	< 150	100	1200
instrins. charge carrier density at 300 K (cm^{-3})	$1.45 \cdot 10^{10}$	$2.4 \cdot 10^{13}$	$2 \cdot 10^{6}$	2		$\approx 10^{-27}$
instrins. resistivity at 300 K (Ω cm)	$2.3 \cdot 10^{5}$	47	$\approx 10^{8}$		$\approx 10^{9}$	$\geq 10^{42}$
Breakdown field (V/cm)	$3 \cdot 10^{5}$	$\approx 10^{5}$	$4 \cdot 10^{5}$	$\approx 10^{6}$		$3 \cdot 10^{7}$
Mean E to create an e^-h^+ pair (eV), 300 K	3.62	2.9	4.2	≈ 7	4.43	13.25

*usually considered an isolator

*usually considered an isolator

Source: http://www.ioffe.rssi.ru/SVA/NSM/Semicond/ ; S.M.Sze, *Physics of Semicon. Devices* , J. Wiley & Sons, 1981,
J. Singh, Electronic & Optoelectronic Properties of Semiconductor Structures, Cambridge University Press, 2003

Are semiconductors good detector material?

A simple calculation for silicon:
Mean ionization energy $\boldsymbol{I_0 = 3.62\ eV}$, *mean energy loss per flight path*
$\boldsymbol{dE/dx = 3.87\ MeV/cm}$.
*Intrinsic charge carrier density at T = 300 K a*ssuming a detector with a thickness of *d = 300 µm and an area of A = 1 cm*^{2}.
$\boldsymbol{n_i \times vol = 1.45 \cdot 10^{10}\ cm^{-3} \times 0.03cm^{\cdot 1} cm^2 \approx 4.35 \cdot 10^8\ e^- h^+}$ **pairs.**
Assuming a detector with a thickness of *d = 300 µm and an area of A = 1 cm*^{2}.
Signal charge:

$$\frac{dE/dx \cdot d}{I_0} = \frac{3.87 \cdot 10^6\,\mathrm{eV/cm} \cdot 0.03\mathrm{cm}}{3.62\,\mathrm{eV}} \approx 3.2 \cdot 10^4\ \mathrm{e^- h^+ - pairs}$$

Number of thermal created $e^- h^+$ pairs are four orders of magnitude larger than signal!!!

Solution : p-n junction.

Extrinsic semiconductors: n and p doping

n doping with an element 5 atom (e.g. **P, As, Sb**). The 5th valence electrons is weakly bound. The doping atom is called **donor.** The released conduction electron leaves a positively charged ion: the effective space charge **N_{eff} is positive**.

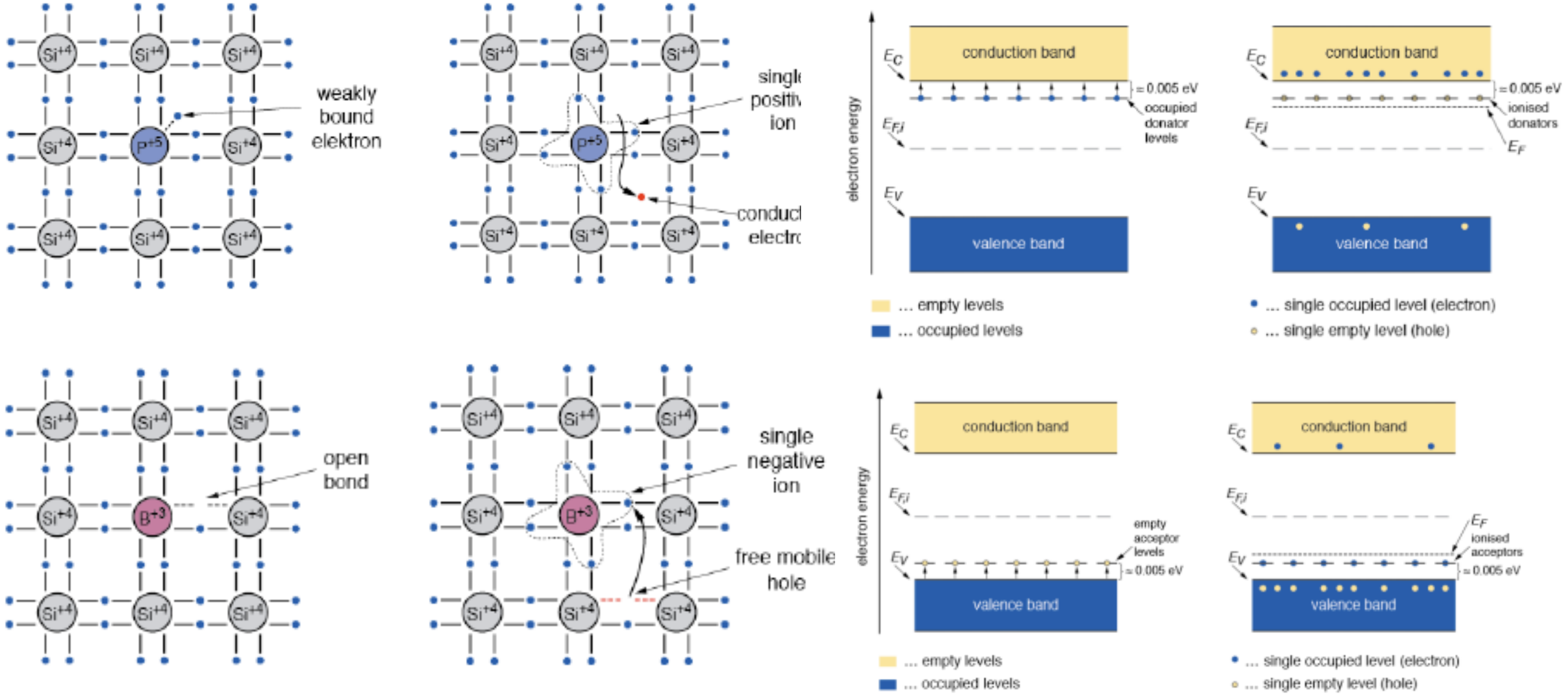

p doping with an element 3 atom (e.g. **B, Al, Ga, In**). One valence bond remains open. This open bond attracts electrons from the neighbour atoms. The doping atom is called **acceptor.** The acceptor atom in the lattice is negatively charged ion: **N_{eff} is negative**.

The p-n junction

At the interface of an n-type and p-type semiconductor the difference in the fermi levels cause diffusion of surplus carries to the other material until thermal equilibrium is reached. At this point the fermi level is equal. The remaining ions create a space charge and an electric field stopping further diffusion.
The stable space charge region is free of charge carries and is called the depletion zone.

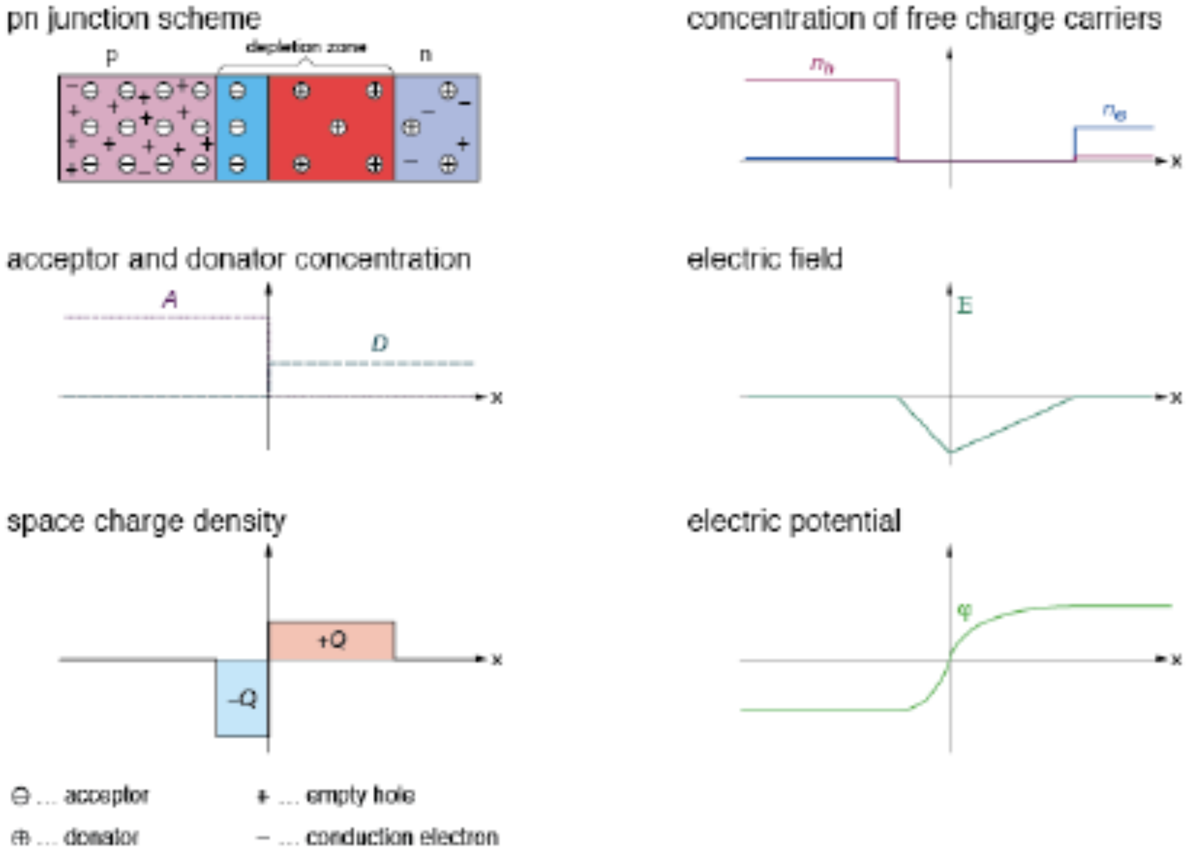

Asimmetric p-n junction: a pad detector

Example of a typical p+-n junction in a silicon detector:
$N_{eff}(p^+) = 10^{15}\ cm^{-3}$, $N_{eff}(d) = 10^{12}\ cm^{-3}$ *(in* n bulk, could be the other way around).
Without external voltage (0.6 V_{BI}):
$W_p = 0.02\ \mu m$
$W_n = 23\ \mu m$
Applying a reverse bias voltage of 100 V:
$W_p = 0.4\ \mu m$
$W_n = 363\ \mu m$

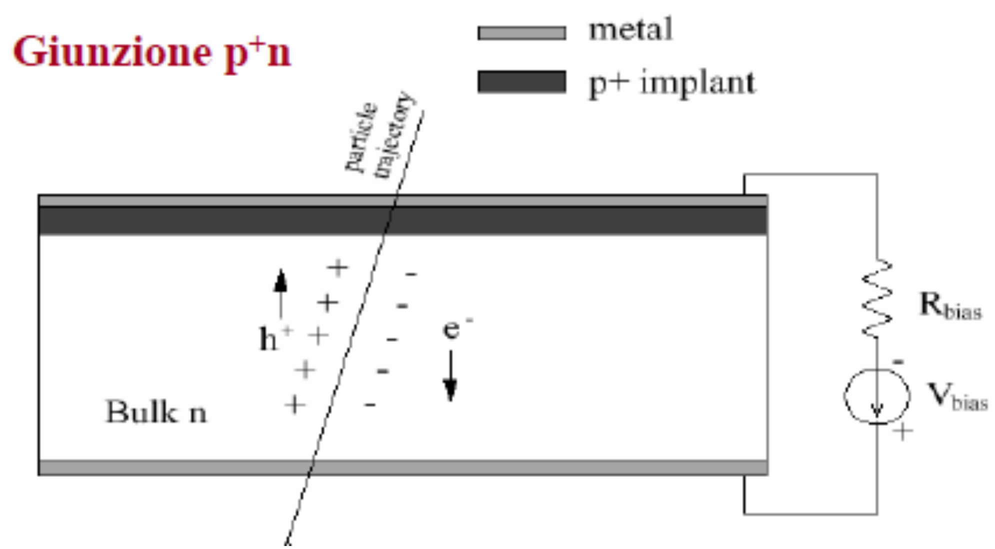

Electrical properties of a diode

Reverse bias junction current

$$J_{inversa} = \frac{1}{2} q \frac{n_i}{\tau_0} W \alpha \sqrt{V_{rev}}$$

Forward bias junction current

$$J_{diretta} \alpha \quad e^{qV/nKT}$$

$$I = I_0 \cdot \left[\exp\left(\frac{eV}{kT}\right) - 1\right]$$

Reverse bias capacitance

$$C = \frac{\varepsilon \cdot Area}{d}$$

Reverse bias depletion depth

$$d = \sqrt{\frac{2\varepsilon}{qN_{eff}}(V_{rev} + V_{built-in})} + L_{diff}$$

Effective space charge

$$N_{eff} = \frac{2 \cdot \varepsilon \cdot (V_{dep} + V_{bi})}{q \cdot W^2}$$

Resistivity

$$\rho = \frac{1}{q \cdot \mu \cdot N_{eff}}$$

Electrical characterisation of a detector

A silicon detector is operated with reverse bias, hence reverse saturation current is relevant (leakage current). This current is dominated by thermally generated e-h+ pair. Due to the applied electric field they cannot recombine and are separated. The drift of the e- and h+ to the electrodes causes the leakage current.

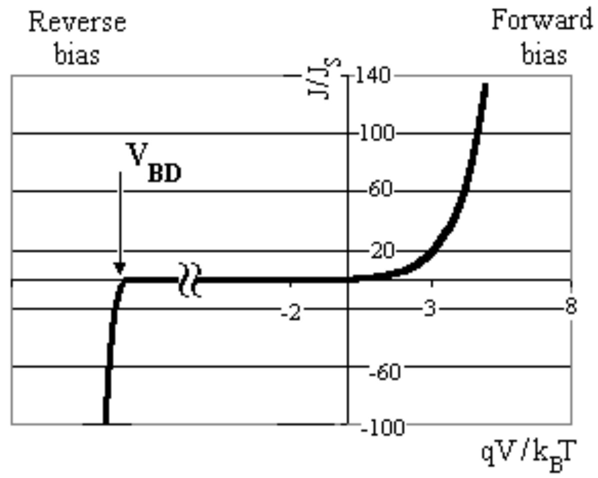

The depletion voltage is the minimum voltage at which the bulk of the sensor is fully depleted. The operating voltage is usually chosen to be slightly higher (overdepletion). High resistivity material (i.e. low doping) requires low depletion voltage.

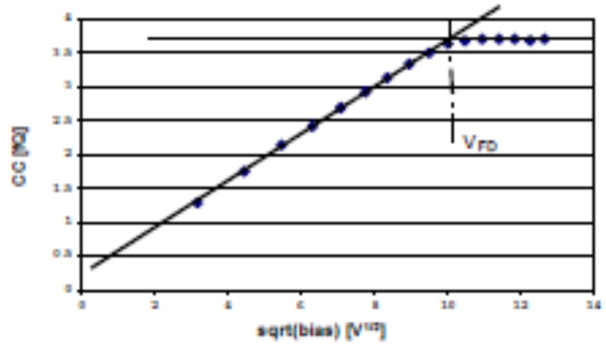

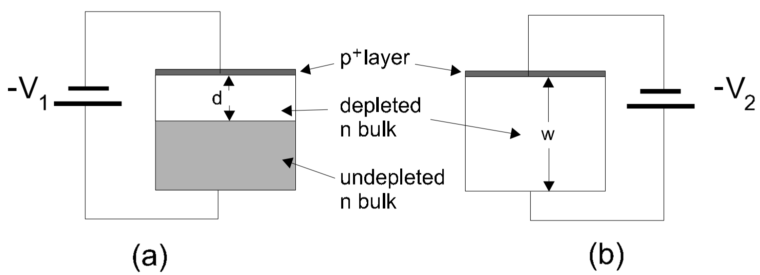

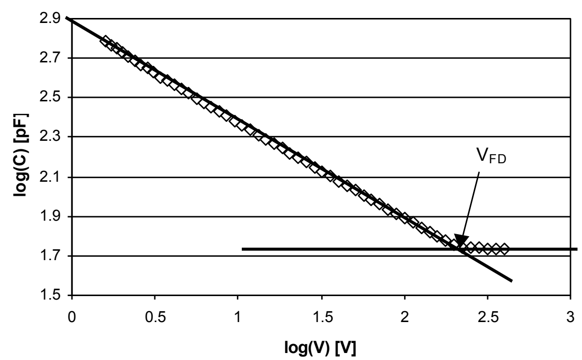

Signal formation

$$\Delta Q = Q\frac{\Delta x}{w}$$ Ramo theorem

$$i_{Te}(t) = \frac{\mu_e}{w}\int_0^w Q(x')(ax'-b)\exp(-\mu_e a t)dx'$$

$$i_{Th}(t) = \frac{\mu_h}{w}\int_0^w Q(ax'-b)\exp(\mu_h a t)dx'$$

$$V(t) = GR_A\int_{-\infty}^{+\infty} i_T(t)dt$$

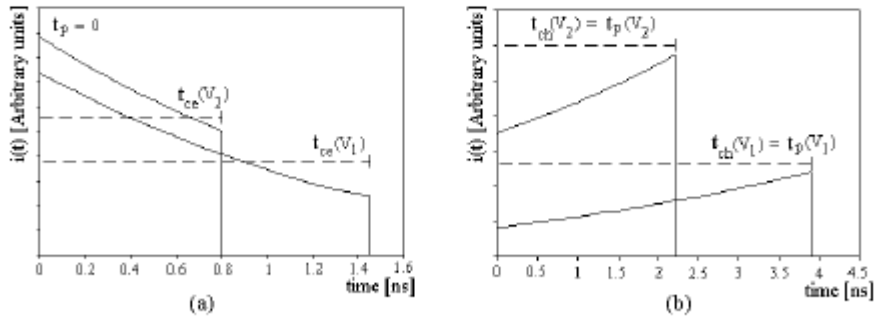

Fig. 4.8 *Ideal pulse shape for (a) electron injection (junction side) and (b) hole injection (ohmic side) of an n-type silicon detector.* $V_{FD} \geq V_1 \geq V_2$.

$$T_{ce} = \frac{1}{a\mu_e}\ln\left(\frac{b}{b-aw}\right) \quad T_{ch} = \frac{1}{a\mu_h}\ln\left(\frac{b}{b-aw}\right) \quad E(x) = -\frac{qN_{eff}}{\varepsilon_{Si}}(x-w) + \frac{V-V_{fd}}{w} = -ax+b$$

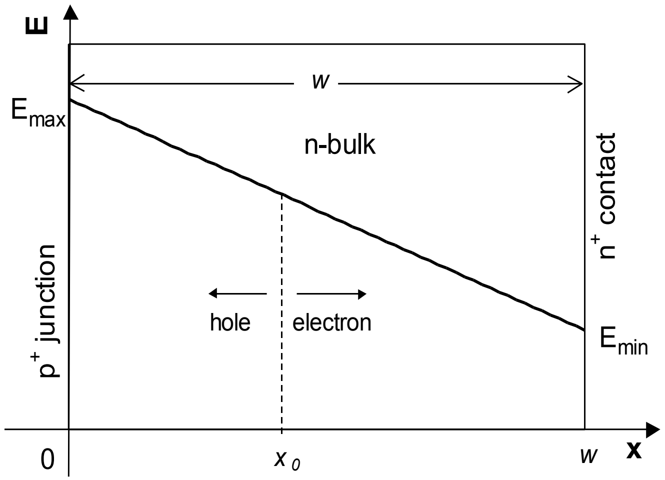

Finally, the detection of a detector!

Short range particles (e.g. α particles, pulsed red light, low energy p .....)

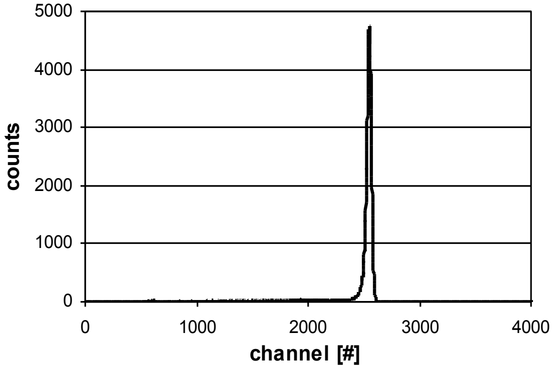

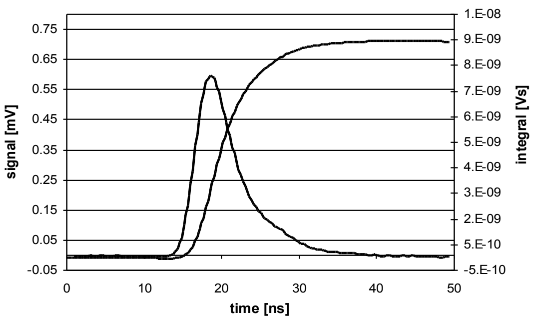

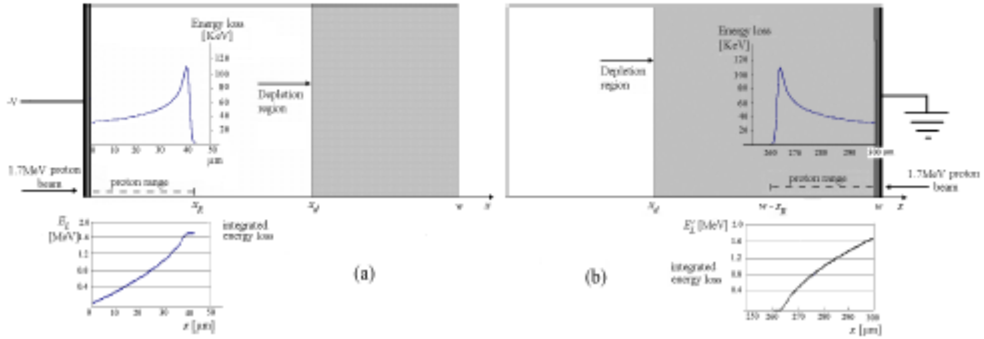

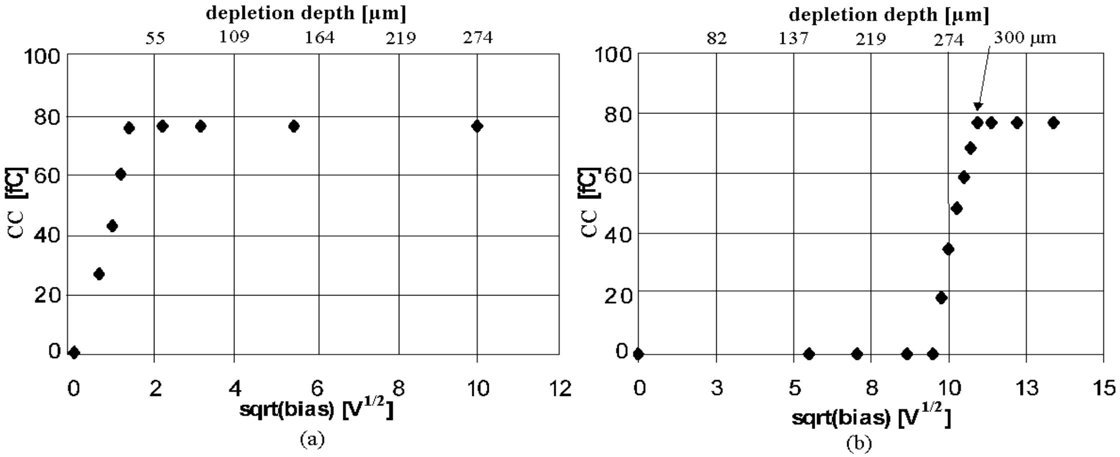

Front (a) and rear (b) illumination with 1.7 MeV protons in a silicon detector with V_{FD} = 120 volts.

Finally, the detection of a detector!

Minimum ionising particles (Landau/Vavilov function)

$$f(\lambda) = \frac{1}{\sqrt{2\pi}} \exp\left(-\frac{1}{2}(\lambda + e^{-\lambda})\right)$$

$$\text{with } \lambda = \frac{\Delta E - \overline{\Delta E}}{C \frac{m_e c^2}{\beta^2} \frac{Zz}{A} \rho \Delta x}$$

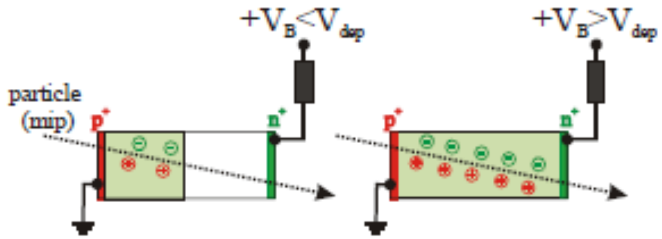

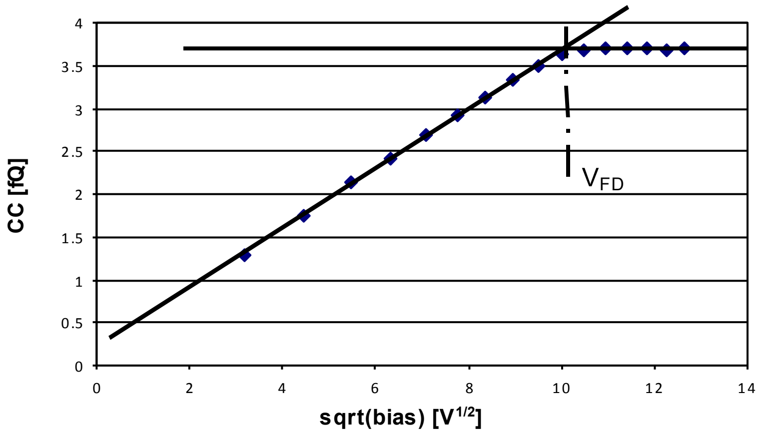

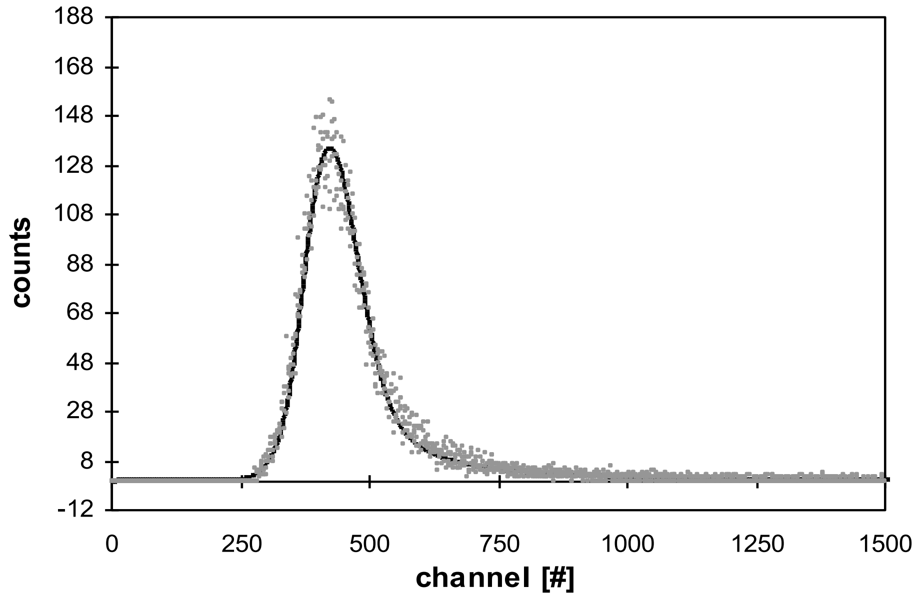

Mip signal: 72 e/μm, 22600 300μm:
Medium signal 300 μm: 32400
(~30% higher).

Finally, the detection of a detector!

High energy photons (x, γ-rays).

Low quantum efficiency (low Z).

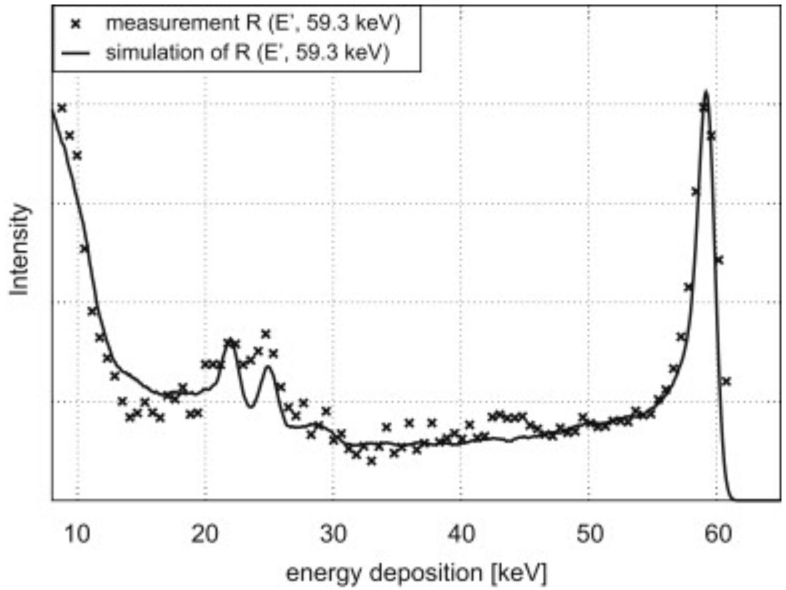

Reconstruction of X-ray spectra with the energy sensitive photon counting detector Medipix2 , T. Michel et al., NIMA 598, 2009.

Electrons from photon interactions deposit energy in silicon.

Fabrication of a segmented silicon detector

1. Starting Point: single-crystal n(p)-doped wafer (ND ≈ 1–5·10^{12} cm^{-3})
2. Surface passivation by SiO_2-layer (approx. 200 nm thick). E.g. growing by (dry) thermal oxidation at 1030 °C.
3. Window opening using **photolithography technique with** etching, e.g. for strips
4. Doping using either
- Thermal diffusion (furnace)
- Ion implantation (p+-strip: Boron, 15 keV,

N_A ≈ 5·10^{16} cm^{-2}; Ohmic backplane: As, B, 30 keV, N_D ≈ 5·10^{15} cm^{-2}.
5. After ion implantation: Curing of damage via thermal annealing at approx. 600°C, (activation of dopant atoms by incorporation into silicon lattice)
6. Metallization of front side: sputtering or CVD
7. Removing of excess metal by photolitography: etching of noncovered areas
8. Full-area metallization of backplane with annealing at approx. 450°C for better adherence between metal and silicon

Last step: wafer dicing (cutting)

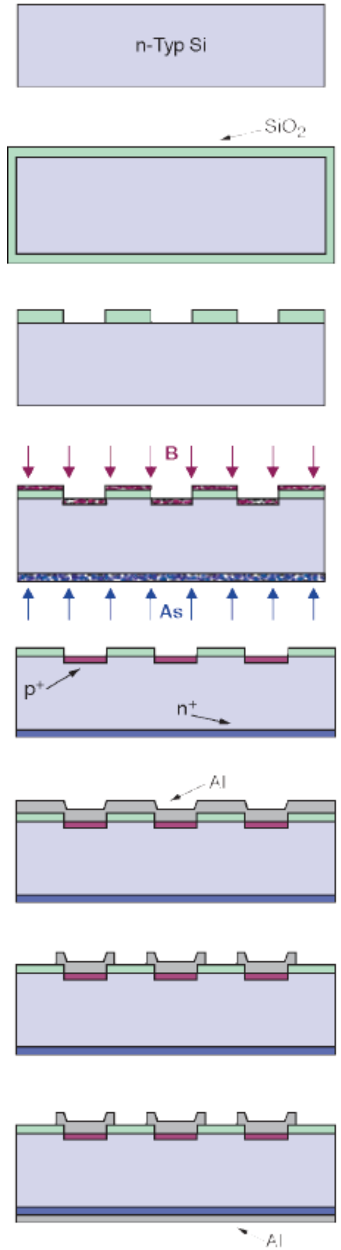

This example: DC coupled microstrip detectors

Photolithography

Quartz mask containing the feature of the segmented detector.

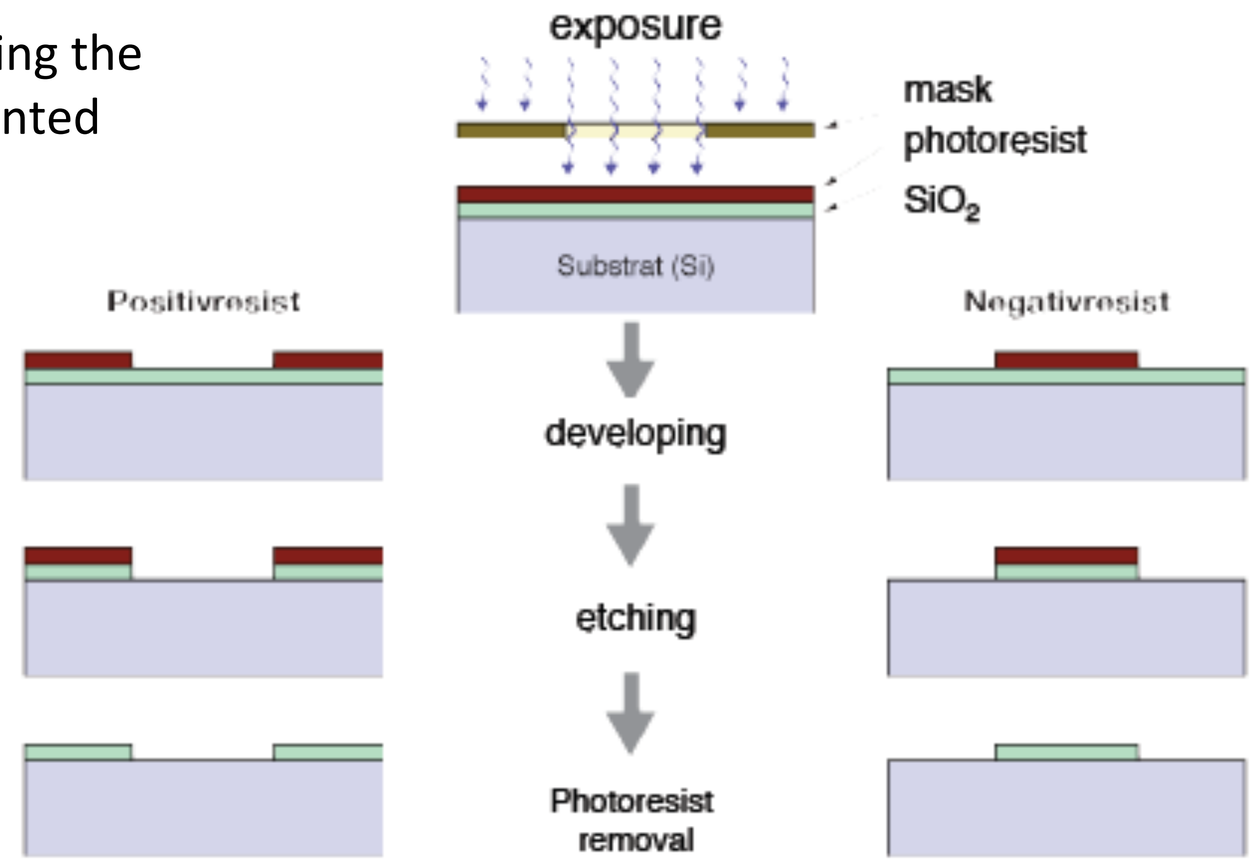

Main properties of segmented silicon sensors

Signal to noise ratio (S/N) (typical case: mip)

Contributions to noise:
Detector leakage current (shot noise): ENC_j
Detector capacitance (serial noise): ENC_C
Detector serial resistance (serial noise): ENC_{RS}
Detector parallel resistance (parallel noise): ENC_{RP}

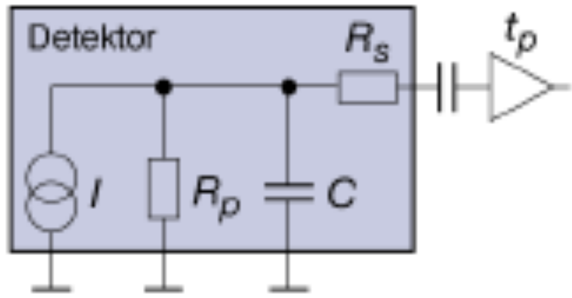

$$ENC_I = \frac{e}{2}\sqrt{\frac{I t_p}{e}}$$

$$ENC_C = a + b \cdot C$$

$$ENC_{Rp} = \frac{e}{e}\sqrt{\frac{kT t_p}{2R_p}}$$

$$ENC_{Rs} \approx 0.395\, C\sqrt{\frac{R_s}{t_p}}$$

$$ENC = \sqrt{ENC_C^2 + ENC_I^2 + ENC_{Rp}^2 + ENC_{Rs}^2}$$

Generally for tracking efficiency close to 100% a S/N ≥ 10 is required. A mip in 300µm thick silicon gives ~ 25000e, make sure noise is adequate.

Signal to Noise ratio Example with diodes

- **Landau distribution has a low energy tail**
  - becomes even lower by noise broadening

What is signal and what is noise?

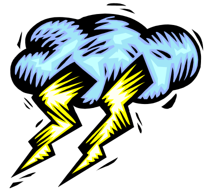

- **Noise sources: (ENC = Equivalent Noise Charge)**

  - Capacitance $$ENC \propto C_d$$

  - Leakage Current $$ENC \propto \sqrt{I}$$

  - Thermal Noise (bias resistor) $$ENC \propto \sqrt{k_B T / R}$$

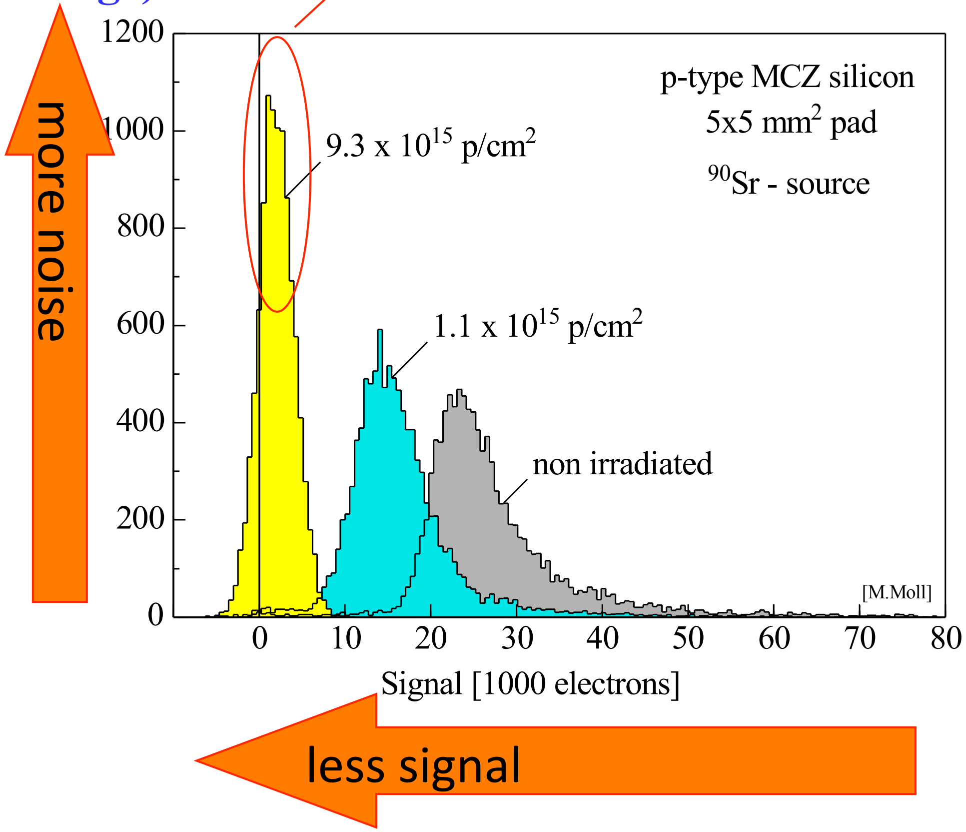

- **Figure of Merit: Signal-to-Noise Ratio S/N. Radiation damage severely degrades the S/N, people get nervous below 10.**

Shot noise and C_{input} noise

Amplifier peaking time (integration time) = t_p

Noise contribution by the leakage current:

$$ENC_I = \frac{e}{2}\sqrt{\frac{It_p}{e}}$$

e = Euler number, e = electron charge,

I = reverse current.

Minimum with low leakage current and short electronics integration time.

The detector capacity at the input of a charge sensitive amplifier is usually the dominant noise source in the detector system.

$$ENC_C = a + b \cdot C$$

Parameter s *a and b are given by the design of the amplifier. C is the detector capacitance at the input of the amplifier channel.*

Typical values are (amplifier with ~ 1 µs integration time): a ≈ 160 e und b ≈ 12 e/pF.

To reduce this noise component segmented detectors with short strip or pixel structures are preferred.

Parallel and series resistor noise

Amplifier peaking time (integration time) = t_p. *e* = Euler number, e = electron charge, k = Boltzmann constant, T = temperature, R_p = parallel resistor.

$$ENC_{Rp} = \frac{e}{e}\sqrt{\frac{kTt_p}{2R_p}}$$

Amplifier peaking time (integration time) = t_p. *e* = Euler number, e = electron charge, k = Boltzmann constant, T = temperature, R_p = parallel resistor. If T = 300 K:

$$ENC \approx 772\sqrt{t_p / Rr_p}$$

(R_p in MΩ, t_p in μs)

To reduce this noise the parallel (bias) resistor should be large!

The series resistor R_s is the resistance of the connection between strips and amplifier input (e.g. aluminium readout lines, hybrid connections, etc.). It can be written as:

$$ENC_{Rs} \approx 0.395\, C\sqrt{\frac{R_s}{t_p}}$$

C is the detector capacitance and R_S the serial resistance. Note that, in this noise contribution *t_p is inverse: long t_p* reduces the noise. The detector capacitance is again responsible for larger noise.

To reduce this noise component aluminium lines should have low resistance.

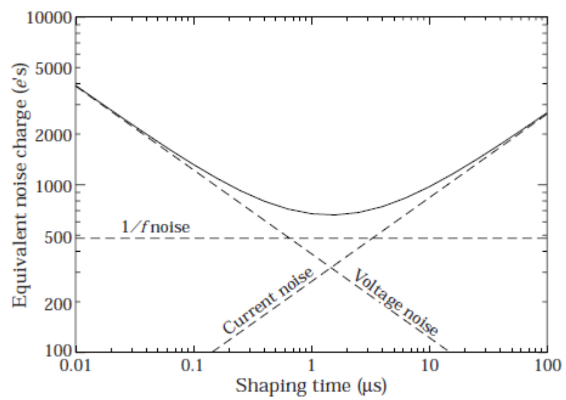

Resolution of segmented detectors

The position resolution is the main parameter of detectors for tracking systems.
It depends on various factors, some due to device physics and some to the design of the system.

Physics processes:

– Statistical fluctuations of the energy loss (contribution of delta rays, will not talk about this)

– Diffusion of charge carriers

External parameter:

– Binary readout (thresh hold counter) or read out of analogue signal value

– Distance between strips (strip pitch)

– Signal to noise ratio

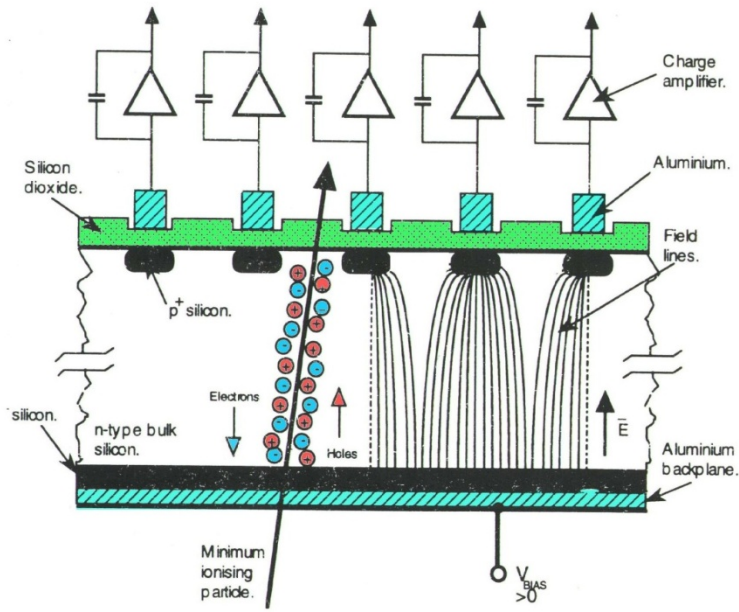

Resolution of segmented detectors

$$\sigma^2 = \frac{\int_{-P/2}^{P/2}(x-c)D(x)dx}{\int_{-P/2}^{P/2}D(x)dx} = \frac{\int_{-P/2}^{P/2}x^2dx}{\int_{-P/2}^{P/2}dx} = \frac{p^2}{12}$$

Binary resolution (can't get worse!):
X = strip position
P = strip pitch (distance between strips)

$$\sigma = \frac{p}{\sqrt{12}}$$

With analogue readout.
Charge centre of gravity between strips:
$x_1, x_2, \ldots x_n$ = position of strip 1, 2 , ..., n
$h_1, h_2, \ldots h_n$ = signal height of strip 1, 2 , ..., n
High resolution (1 μm) possible

$$\sigma_x \propto p/(S/N)$$

Diffusion

After the ionizing particle has passed the detector the e^+h^- pairs are close to the original track. While the cloud of e+ and h- drift to the electrodes, diffusion widens the charge carrier distribution. After the drift time *t the width (rms) of the* distribution is:

σ_D width of the charge carrier distribution
t drift time
D diffusion coefficient
k Boltzmann constant
T temperature
e electron charge
μ charge carrier mobility

$$\sigma_D = \sqrt{2Dt} \qquad \text{with:} \qquad D = \frac{kT}{e}\mu$$

Note: *$D \propto \mu$ and $t \propto 1/\mu$, hence σ_D is equal for e^- and h^+.*

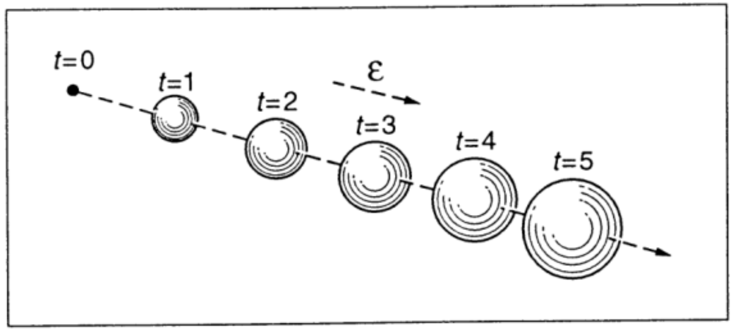

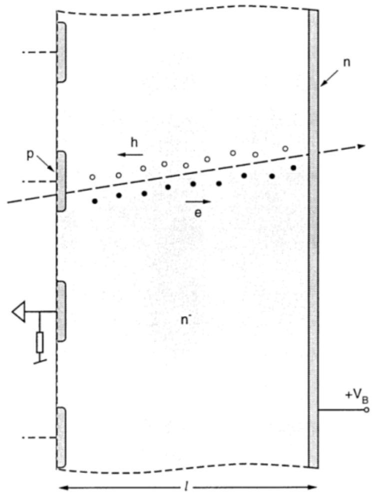

Diffusion widens the charge cloud➔ charge is distributed over more than one strip.
With interpolation (calculation of the charge centre of gravity) a better resolution.
This is only possible if analogue read out of the signal is implemented.
Interpolation is more precise the larger the signal to noise ratio is. Strip pitch and signal to noise ratio determine the position resolution.

Other effects on resolution of segmented detectors systems

Multiple Scattering (MS)

Particles don't only loose energy …

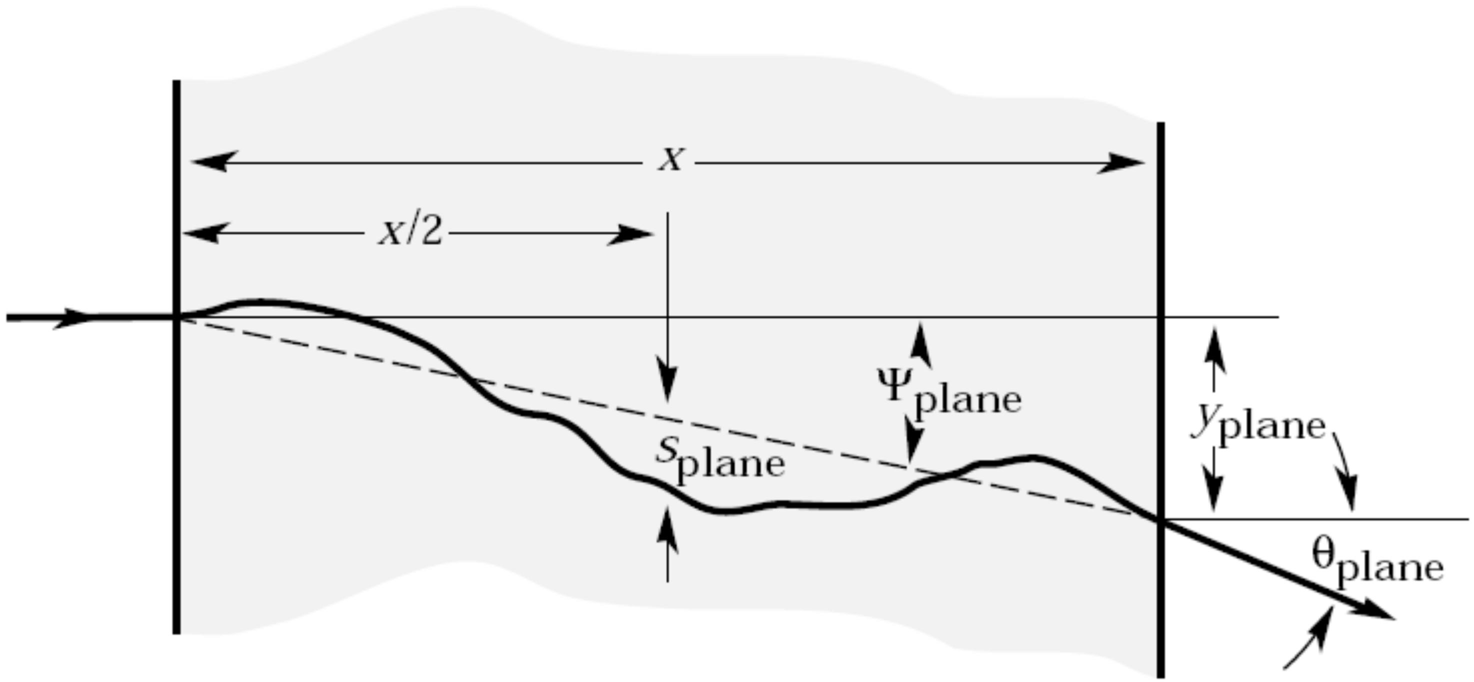

… they also change direction

MS Theory

- Average scattering angle is roughly Gaussian for small deflection angles
- With

$$\theta_0 = \frac{13.6\text{ MeV}}{\beta c p} z \sqrt{\frac{x}{X_0}}\left[1+0.038\ln\left(\frac{x}{X_0}\right)\right]$$

$$X_0 \equiv \text{ radiation length}$$

$$\frac{1}{X_0} = 4\alpha r_e^2 \frac{N_A}{A}\left\{Z^2\left[L_{\rm rad} - f(Z)\right] + Z\,L'_{\rm rad}\right\}$$

Angular distributions are given by

$$\frac{dN}{d\Omega} \propto \frac{1}{2\pi\theta_0^2}\exp\left(-\frac{\theta_{space}^2}{2\theta_0^2}\right)$$

$$\frac{dN}{d\theta_{plane}} \propto \frac{1}{\sqrt{2\pi}\theta_0}\exp\left(-\frac{\theta_{plane}^2}{2\theta_0^2}\right)$$

Element	Z	$L_{\rm rad}$	$L'_{\rm rad}$
H	1	5.31	6.144
He	2	4.79	5.621
Li	3	4.74	5.805
Be	4	4.71	5.924
Others	> 4	$\ln(184.15\,Z^{-1/3})$	$\ln(1194\,Z^{-2/3})$

Various silicon sensors: hybrid pixels

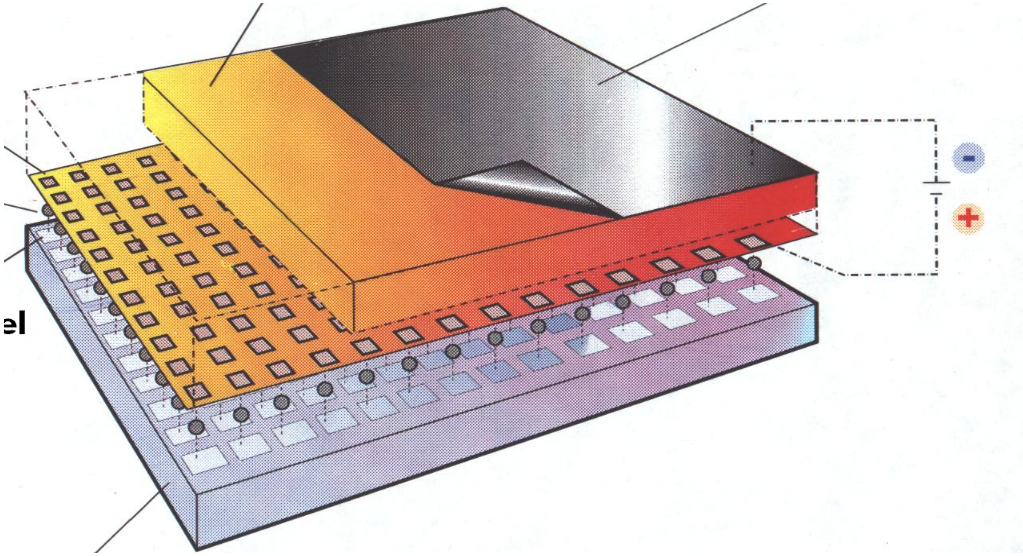

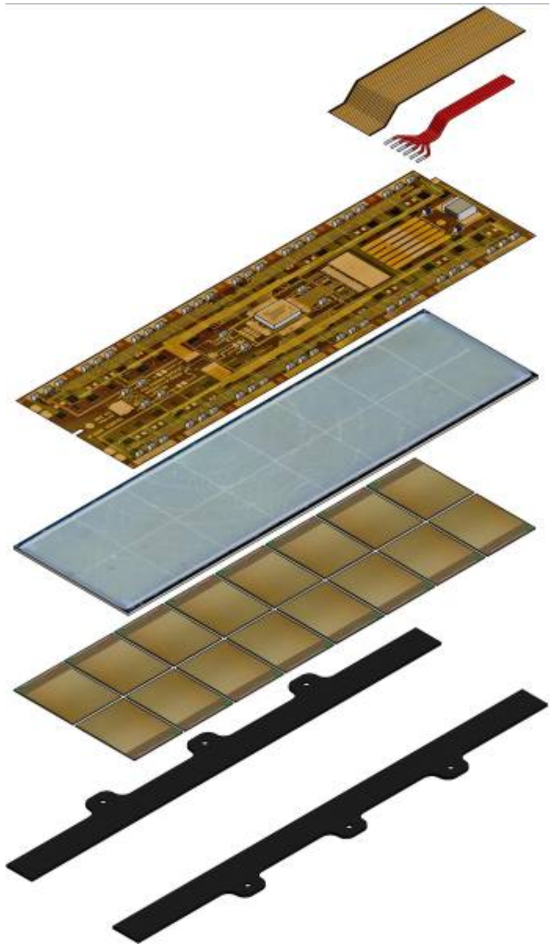

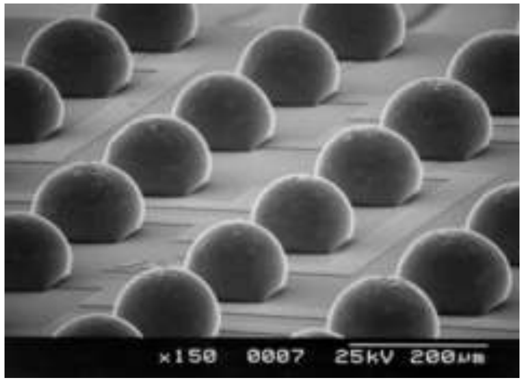

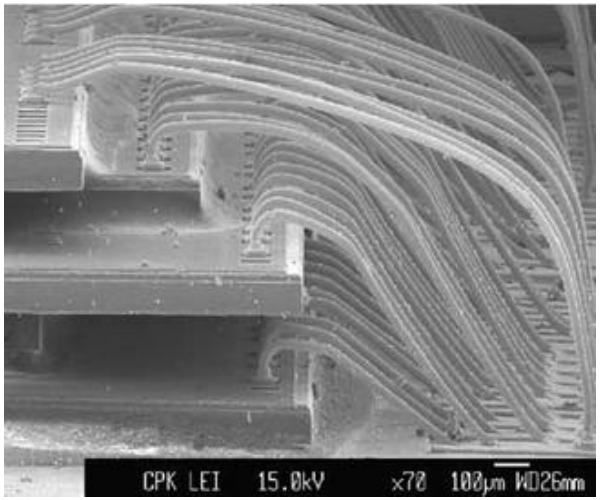

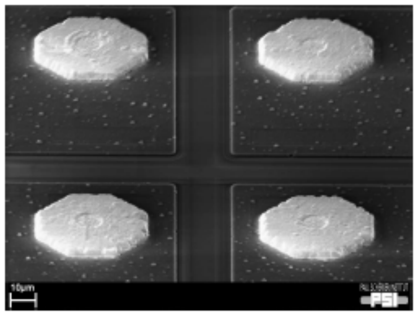

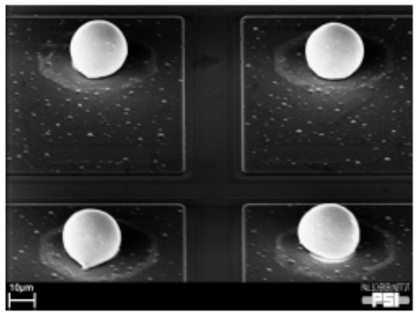

Various silicon sensors: SDD

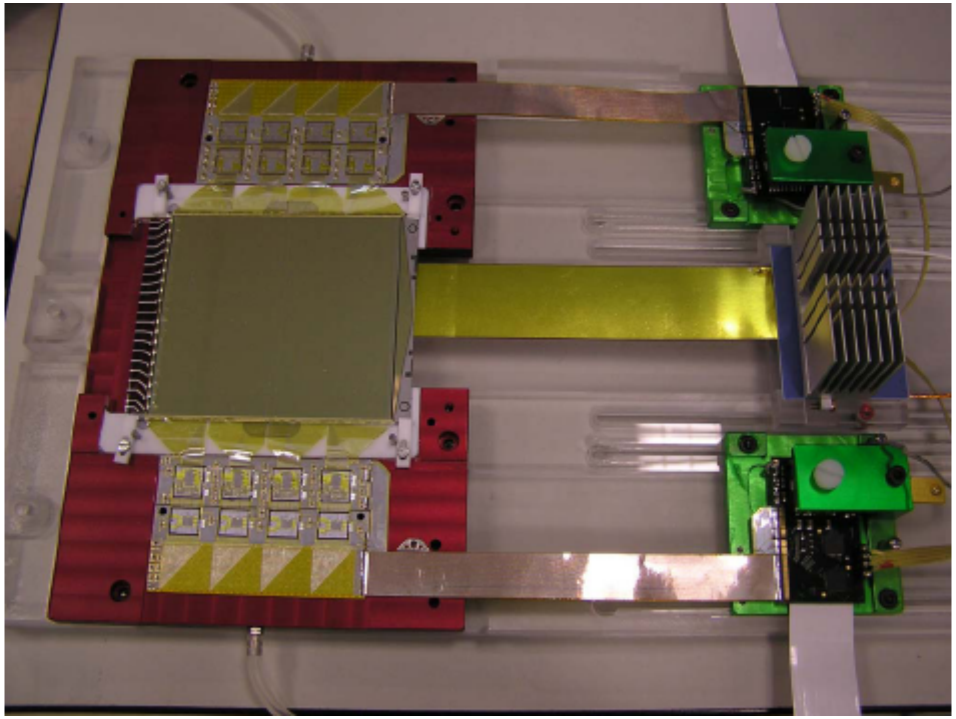

Silicon Drift Detector
(Used e.g. in ALICE)

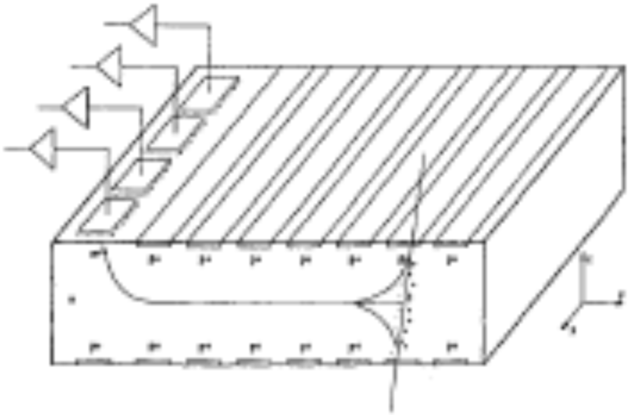

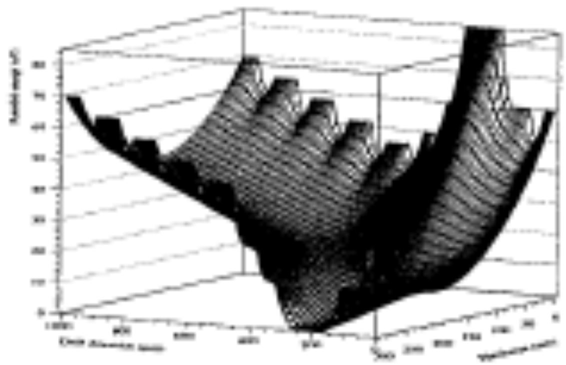

Charged Coupled Devices

The CCD was invented in 1969 by W.S. Boyle and G.E. Smith of the Bell Laboratory. They were not interested in astronomical detectors (and were, in fact, investigating techniques for possible use in a `picture-phone'). Indeed, most of the applications of CCDs are not astronomical. CCDs were first used in astronomy in 1976 when J. Janesick and B. Smith obtained images of Jupiter, Saturn and Uranus using a CCD detector attached to the 61-inch telescope on Mt Bigelow in Arizona. CCDs were rapidly adopted in astronomy and are now ubiquitous: they are easily the most popular and widespread imaging devices used at optical and near infrared wavelengths.

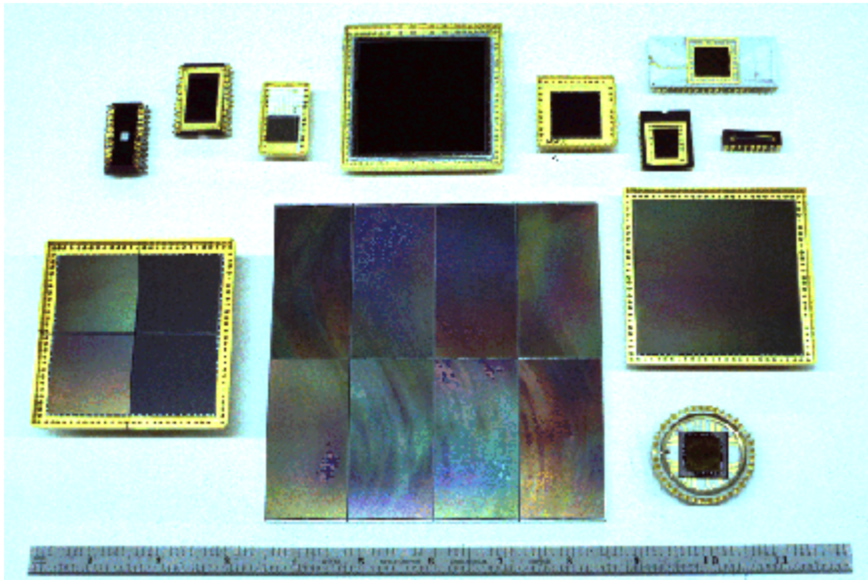

Charged Coupled Devices

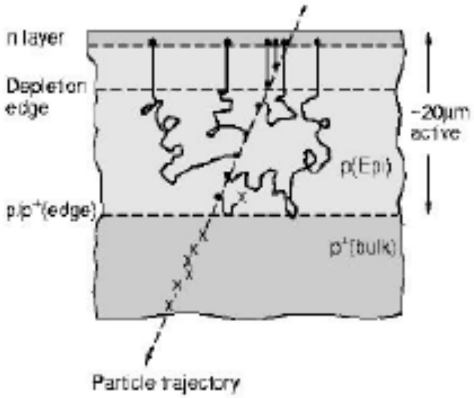

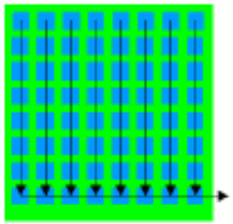

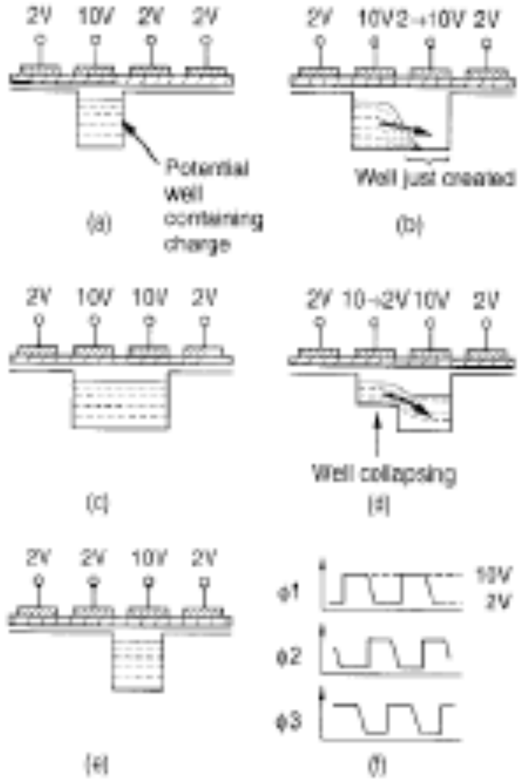

Shallow depletion layer (typically 15 µm), relatively small signal, the charge is kept in the pixel and during readout shifted through the columns and through final row to a single signal readout channel.

DEPFET Pixel Detectors

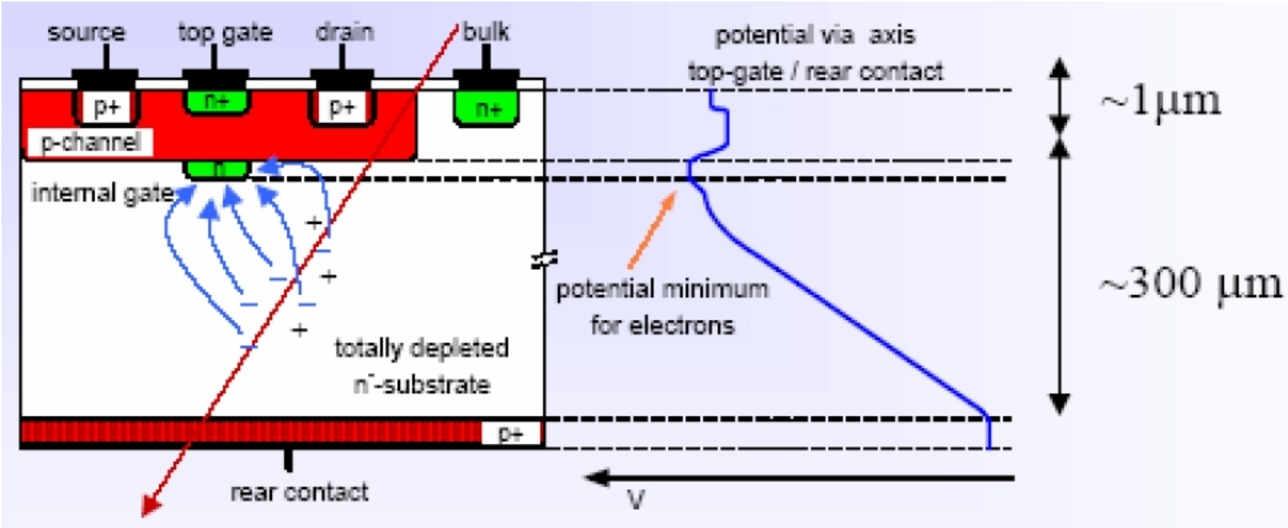

The DEPFET detector is a detector with internal amplification. The n-bulk is fully depleted with a potential minimum below the strips and the structure of a field effect transistor. The electrons created by a charged particle accumulate in the potential minimum. The field configuration is such that the electrons drift underneath the gate of the transistor modifying the source drain current. An active clear is necessary to remove the electrons.

Avalanche Photo Diode and Silicon Photo Multipliers

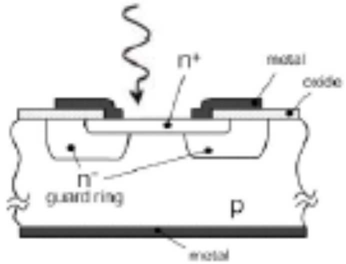

R. H. Haitz, J. App.Phys. Vol. 36, No. 10 (1965) 3123

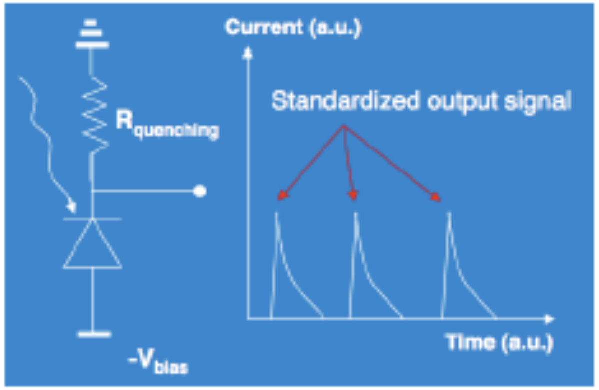

APD are operated in reverse bias mode in breakdown regime. A photon triggers an avalanche breakdown. The large current increase has to be limited by a quenching resistor.

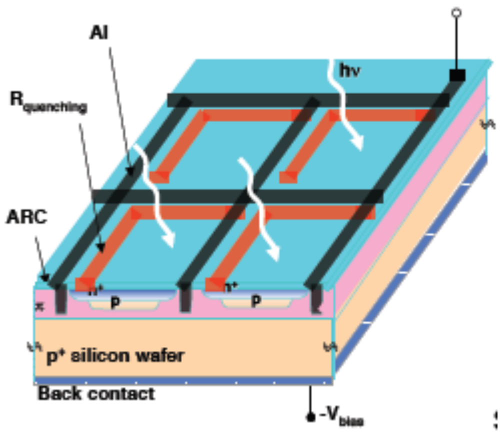

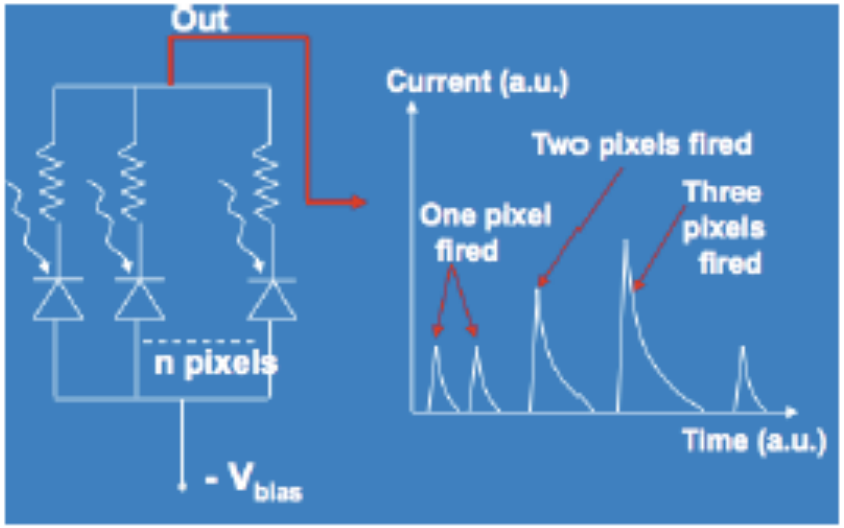

3D (Column) Sensors

S.I. Parker, C.J. Kenney and J. Segal NIM A 395 (1997) 328

3D detectors are non planar. Deep holes are etched into the silicon and filled with n+ and p+ material. Depletion is sideways. The distances between the electrodes are small, hence depletion voltage can be much smaller and charge carries travel much short distances.

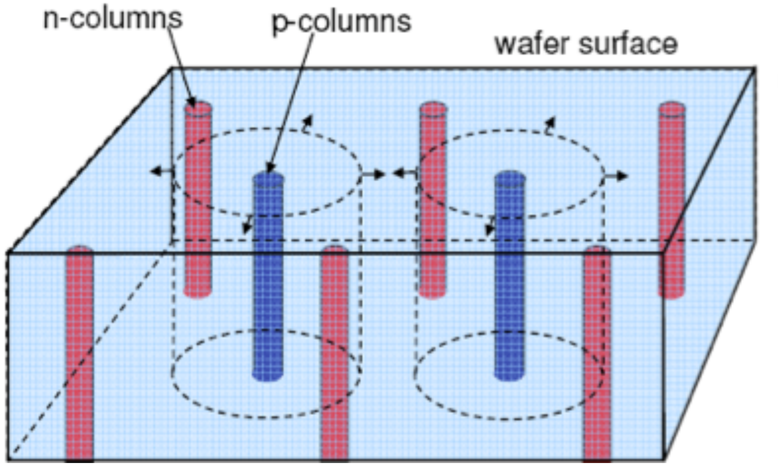

Columns: 10 µm
Pitch: 50 - 100 µm

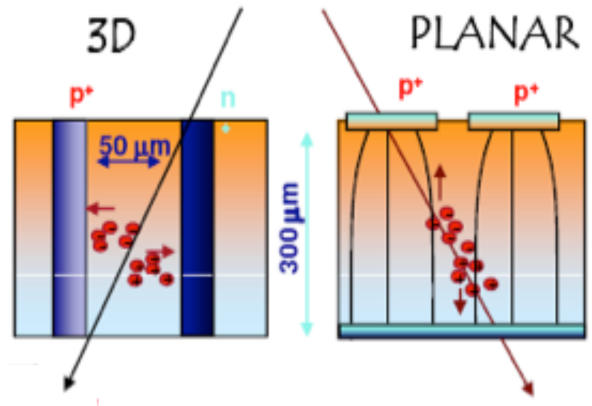

Monolithic Active Pixels

MAPs, **standard CMOS processing**. Active pixel cell with an NMOS transistor. The N-well collects electrons from both ionization and photo-effect.

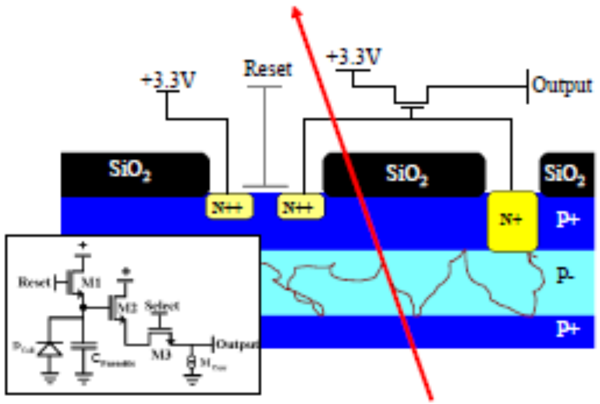

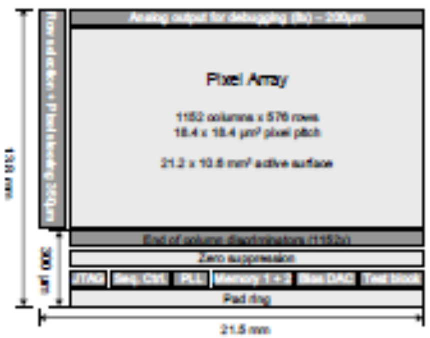

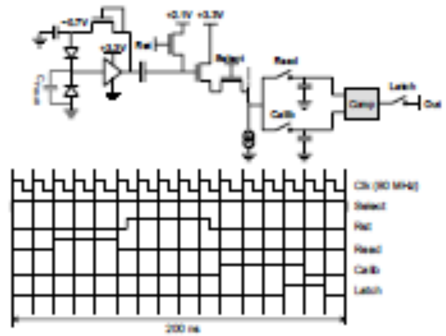

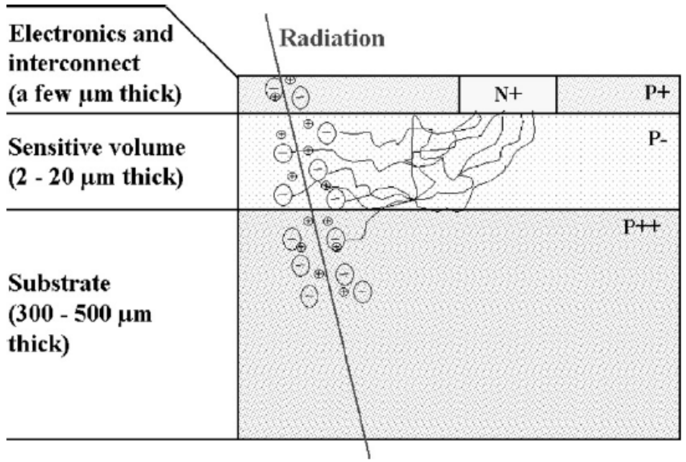

Monolithic Active Pixels

SOI: silicon on insulator

A SOI detector consists of a thick full depleted high resitivity bulk and separated by a layer of SiO2 a low resistivity n-type material. NMOS and PMOs transistors are implemented in the low resitivity material using standard IC methods.

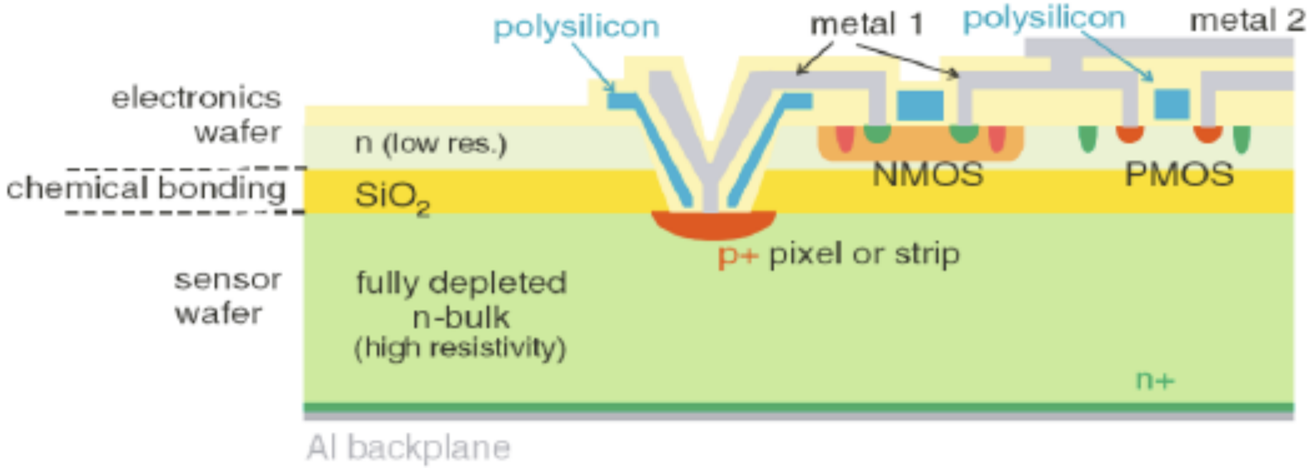

Tracking systems in particle physics

Designing a system:

S/N (for the entire duration of the experiment)

Resolution

Occupancy (readout speed, granularity of the sensors)

Tracking efficiency ~ 100%, fake rate ~ 0.

A very complex example: LHC experiments!!

The Large Hadron Collider Accelerator

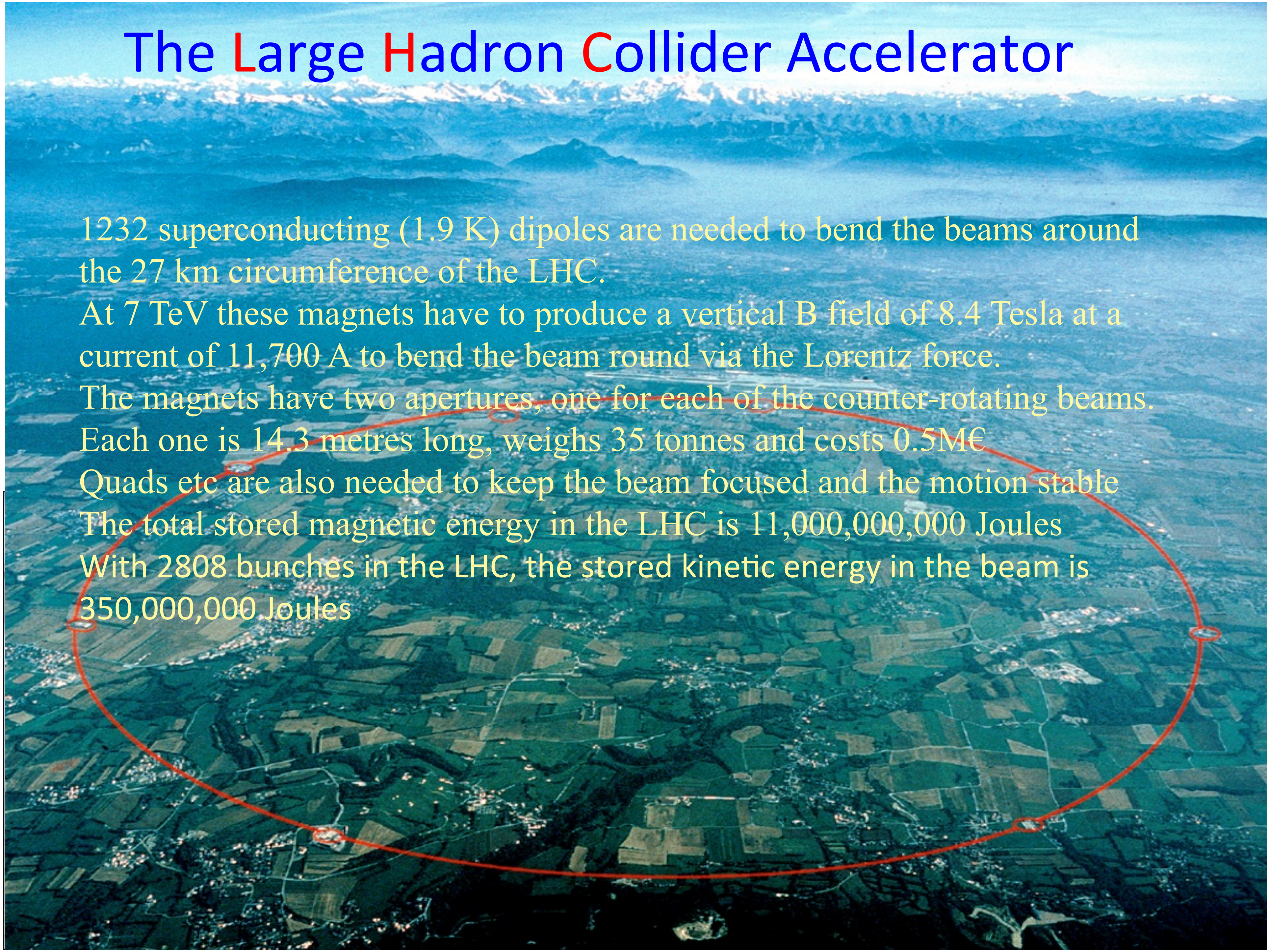

1232 superconducting (1.9 K) dipoles are needed to bend the beams around the 27 km circumference of the LHC.
At 7 TeV these magnets have to produce a vertical B field of 8.4 Tesla at a current of 11,700 A to bend the beam round via the Lorentz force.
The magnets have two apertures, one for each of the counter-rotating beams.
Each one is 14.3 metres long, weighs 35 tonnes and costs 0.5M€
Quads etc are also needed to keep the beam focused and the motion stable
The total stored magnetic energy in the LHC is 11,000,000,000 Joules
With 2808 bunches in the LHC, the stored kinetic energy in the beam is 350,000,000 Joules

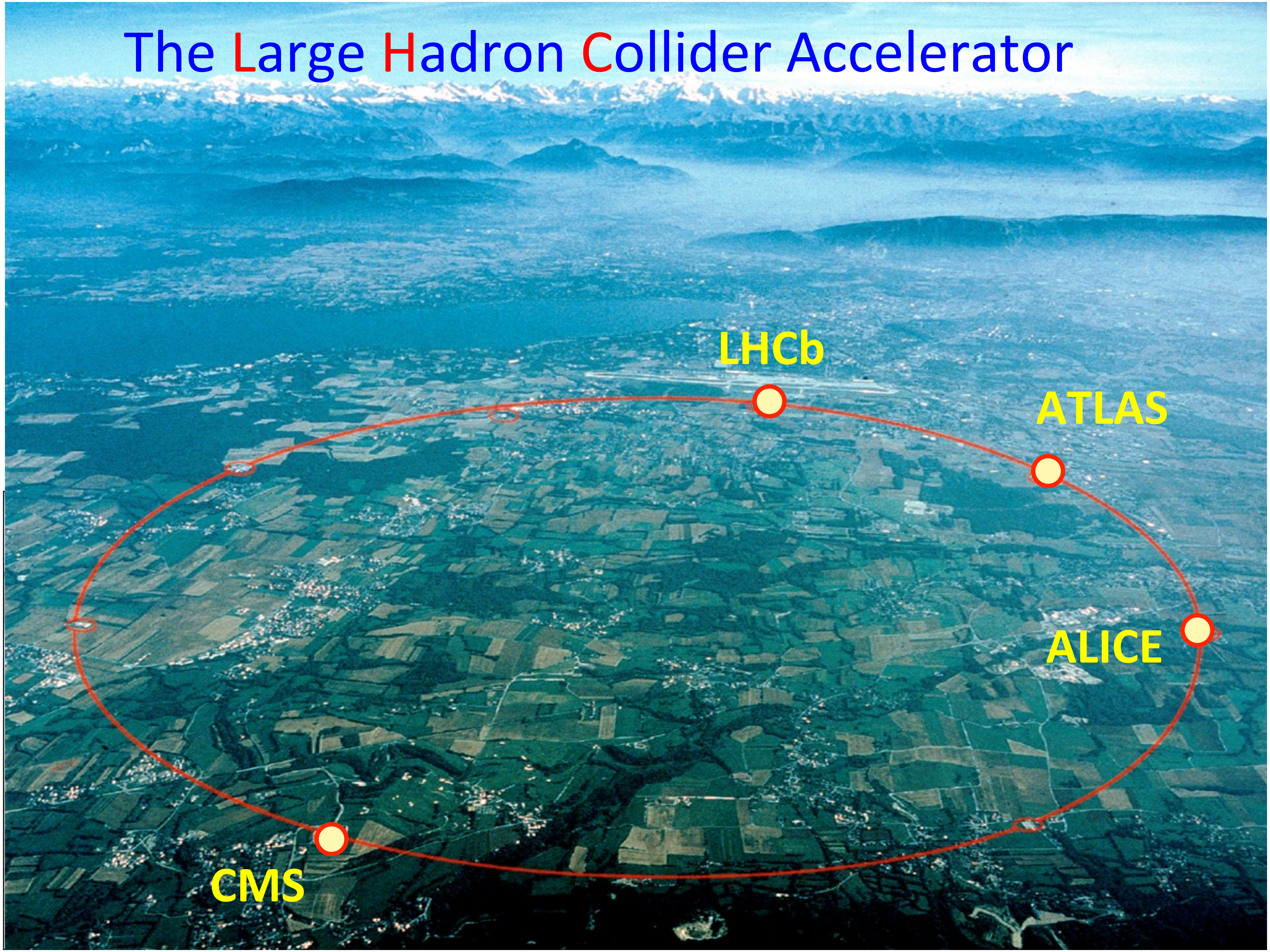
The Large Hadron Collider Accelerator
LHCb
ATLAS
ALICE
CMS

Experiments at the LHC

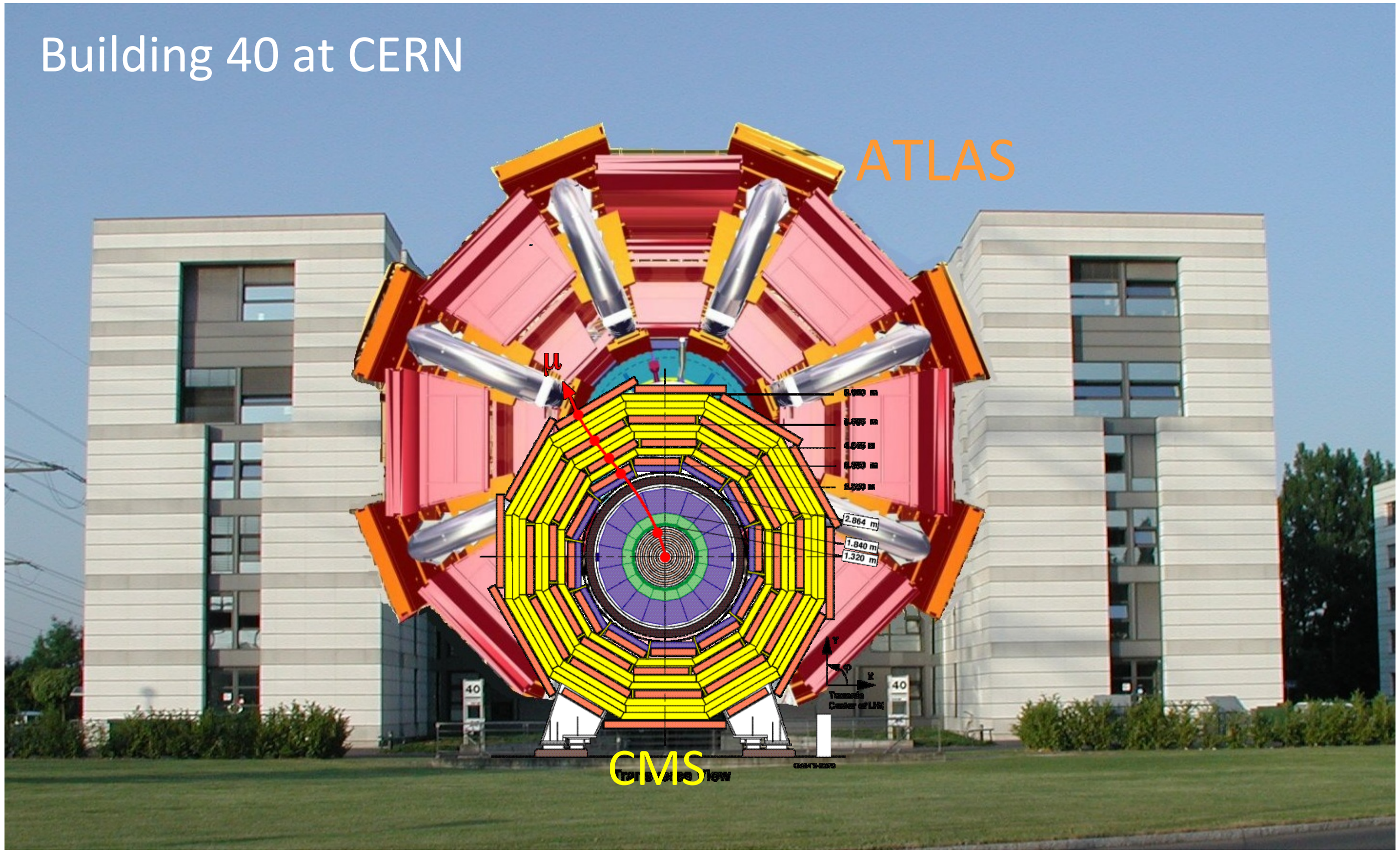

- **ATLAS, CMS, ALICE and LHCb**
- **Detector Technologies**
  - **Noble gases, scintillators, crystals, Cherenkov, …**
  - **Silicon Micro-strip Tracking Detectors**

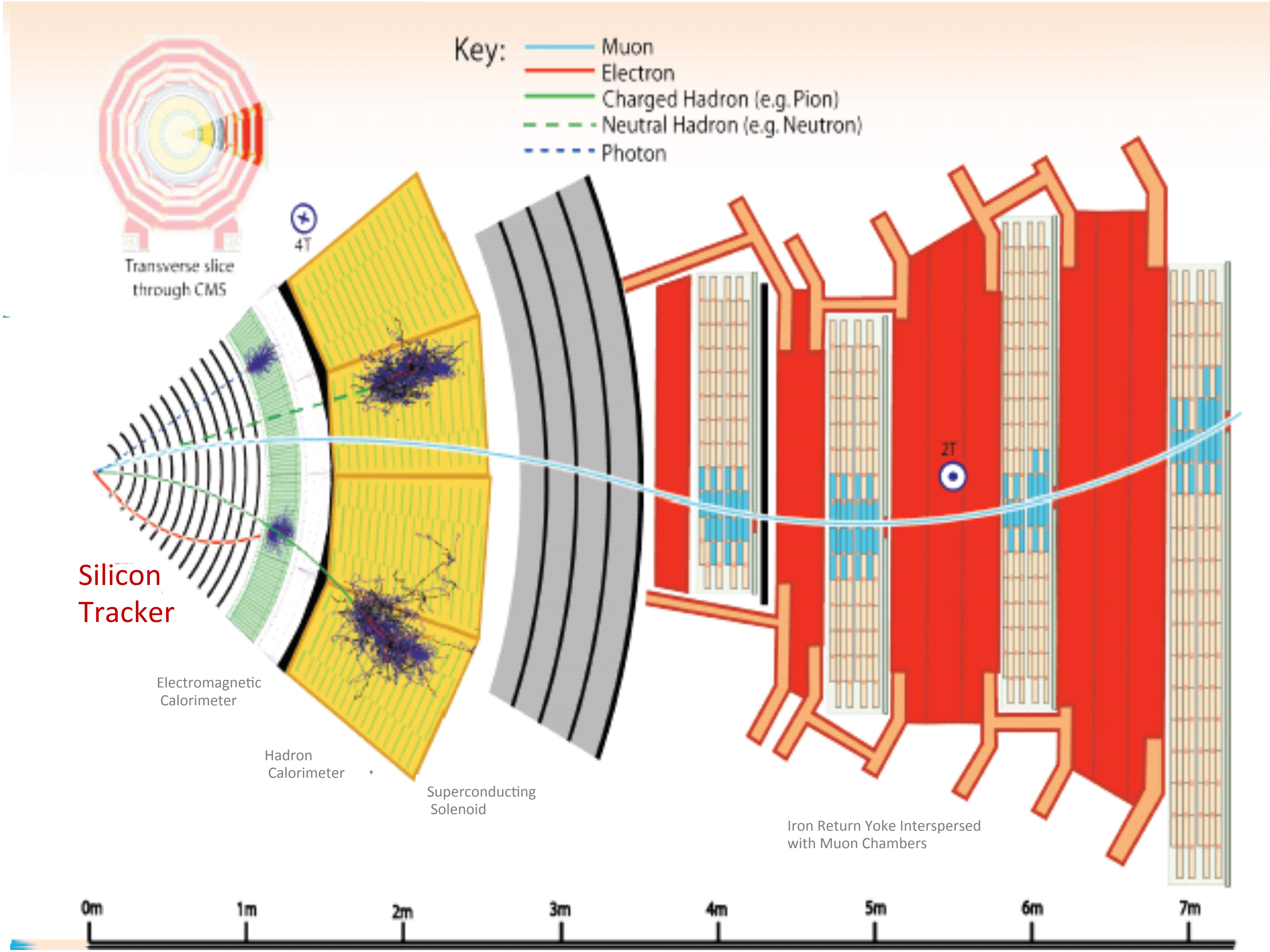
Key:
Muon
Electron
Charged Hadron (e.g. Pion)
Neutral Hadron (e.g. Neutron)
Photon
Transverse slice through CMS
4T
2T
Silicon Tracker
Electromagnetic Calorimeter
Hadron Calorimeter
Superconducting Solenoid
Iron Return Yoke Interspersed with Muon Chambers
0m
1m
2m
3m
4m
5m
6m
7m

ATLAS Silicon Detector Tracker

61m² of silicon micro-strip detectors
~20,000 separate sensors ordered

2112 Barrel and 1976 End-Cap Double-Sided Modules

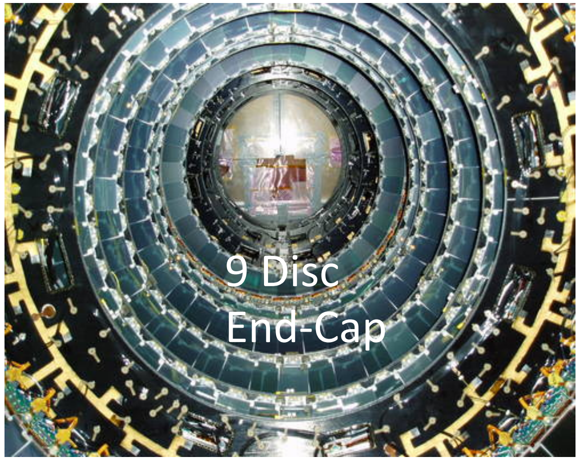

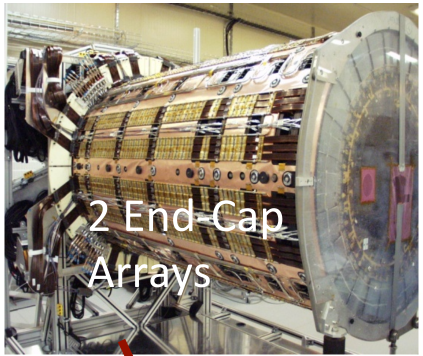

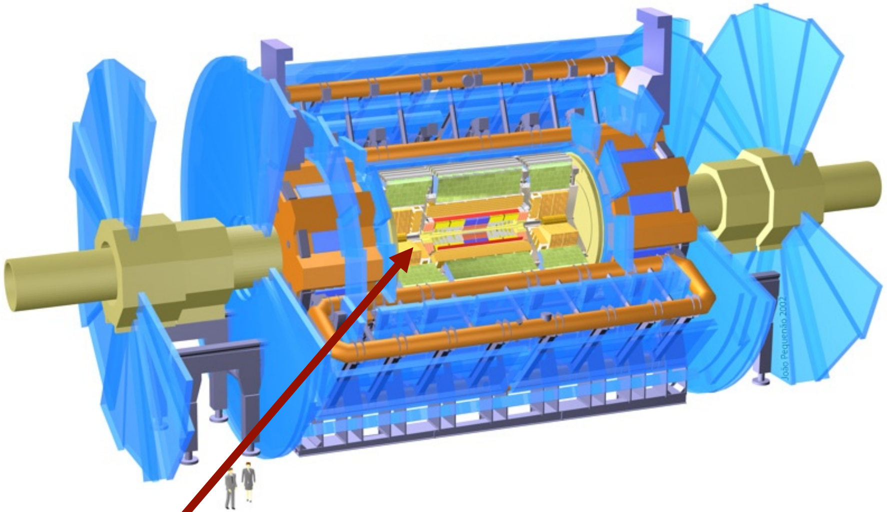

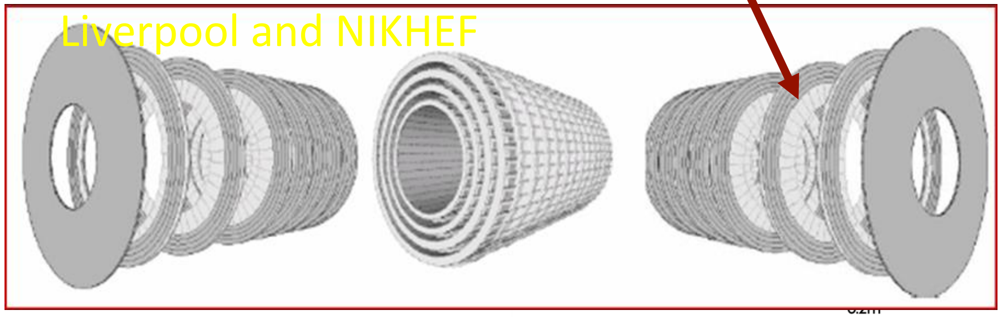

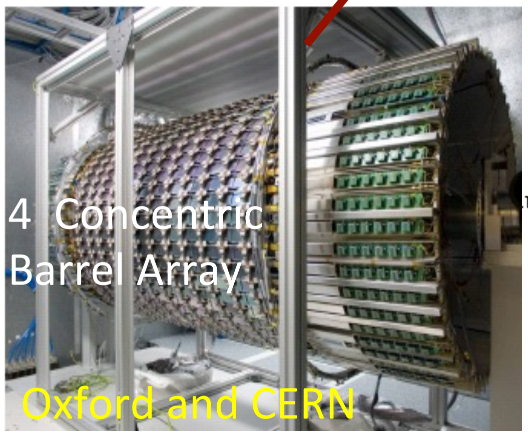

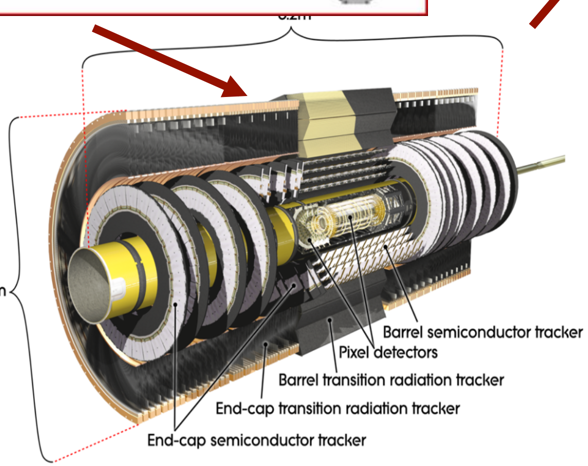

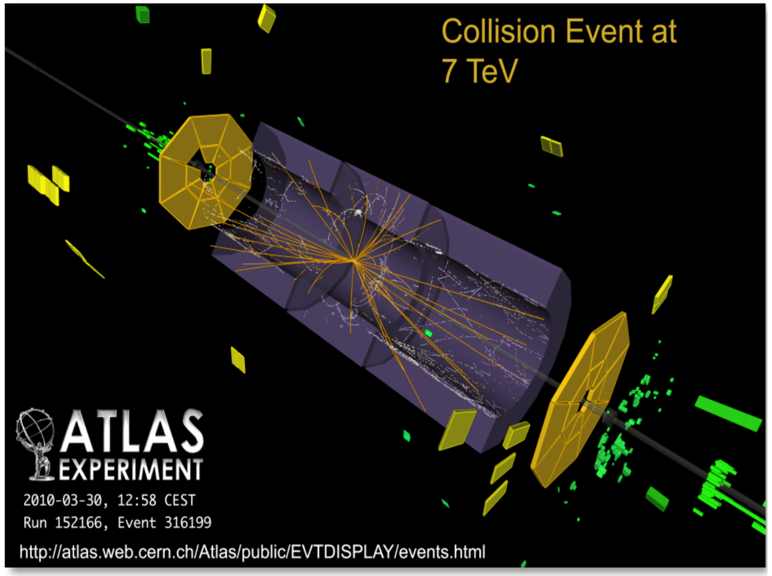

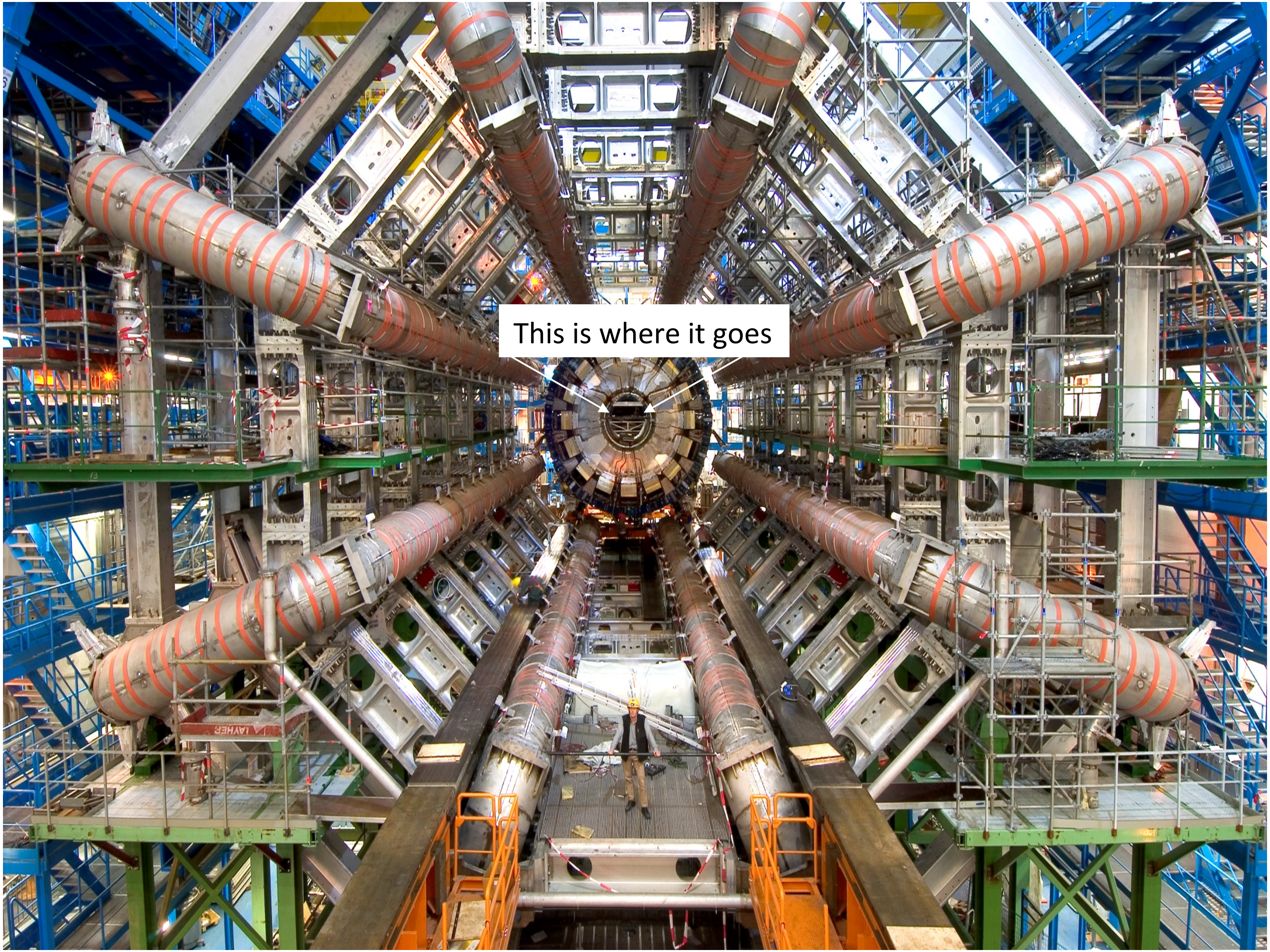
This is where it goes

Installation in ATLAS

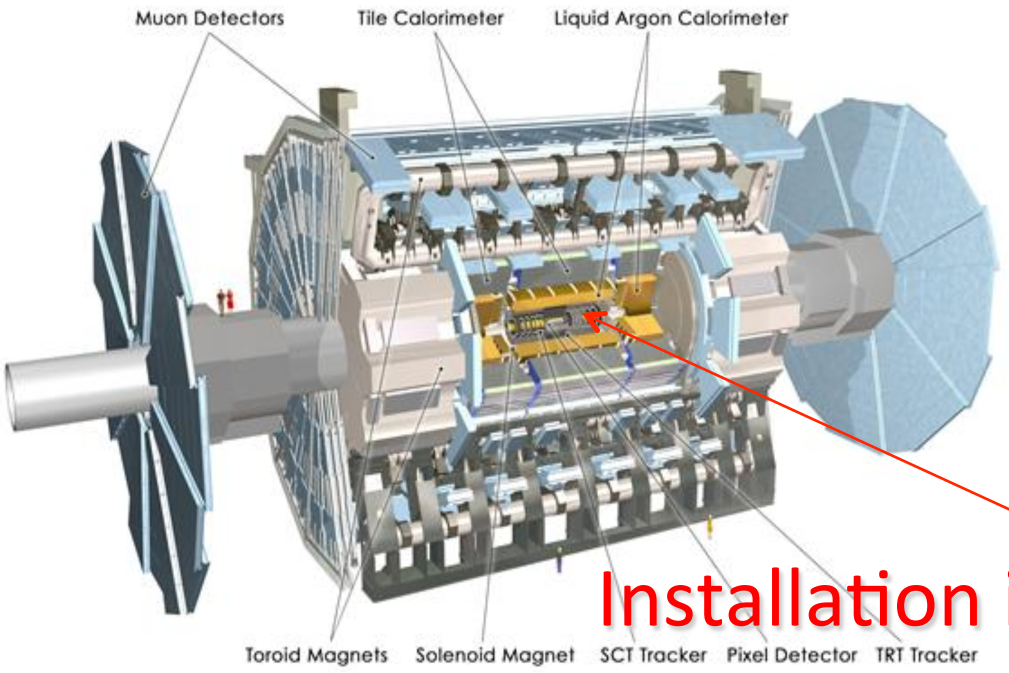

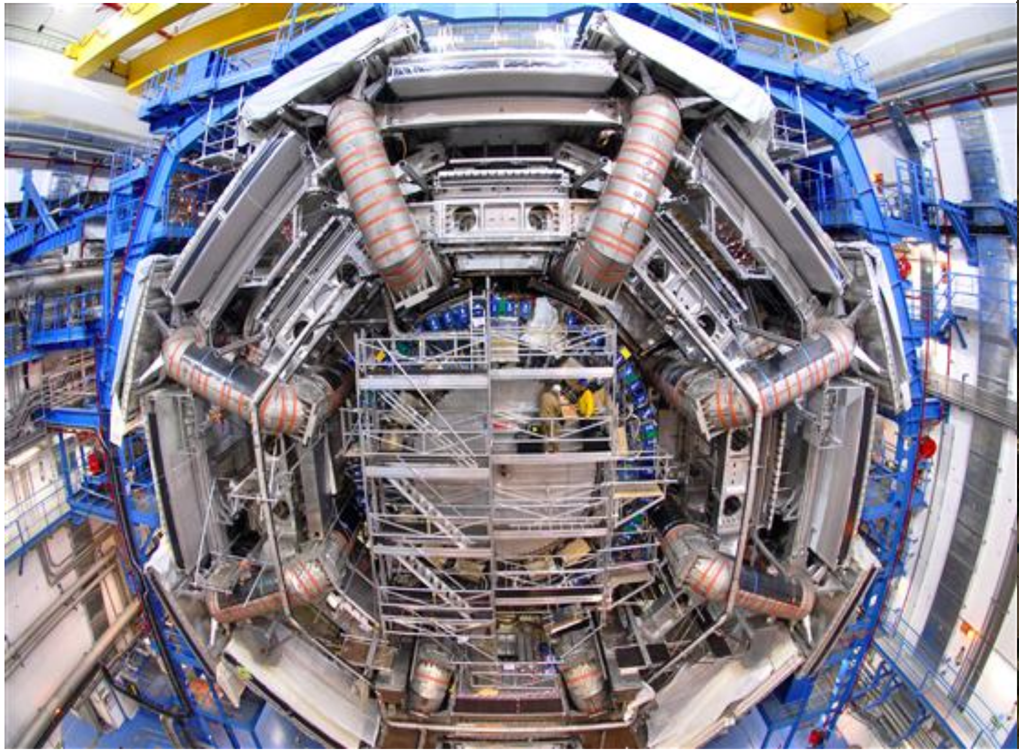

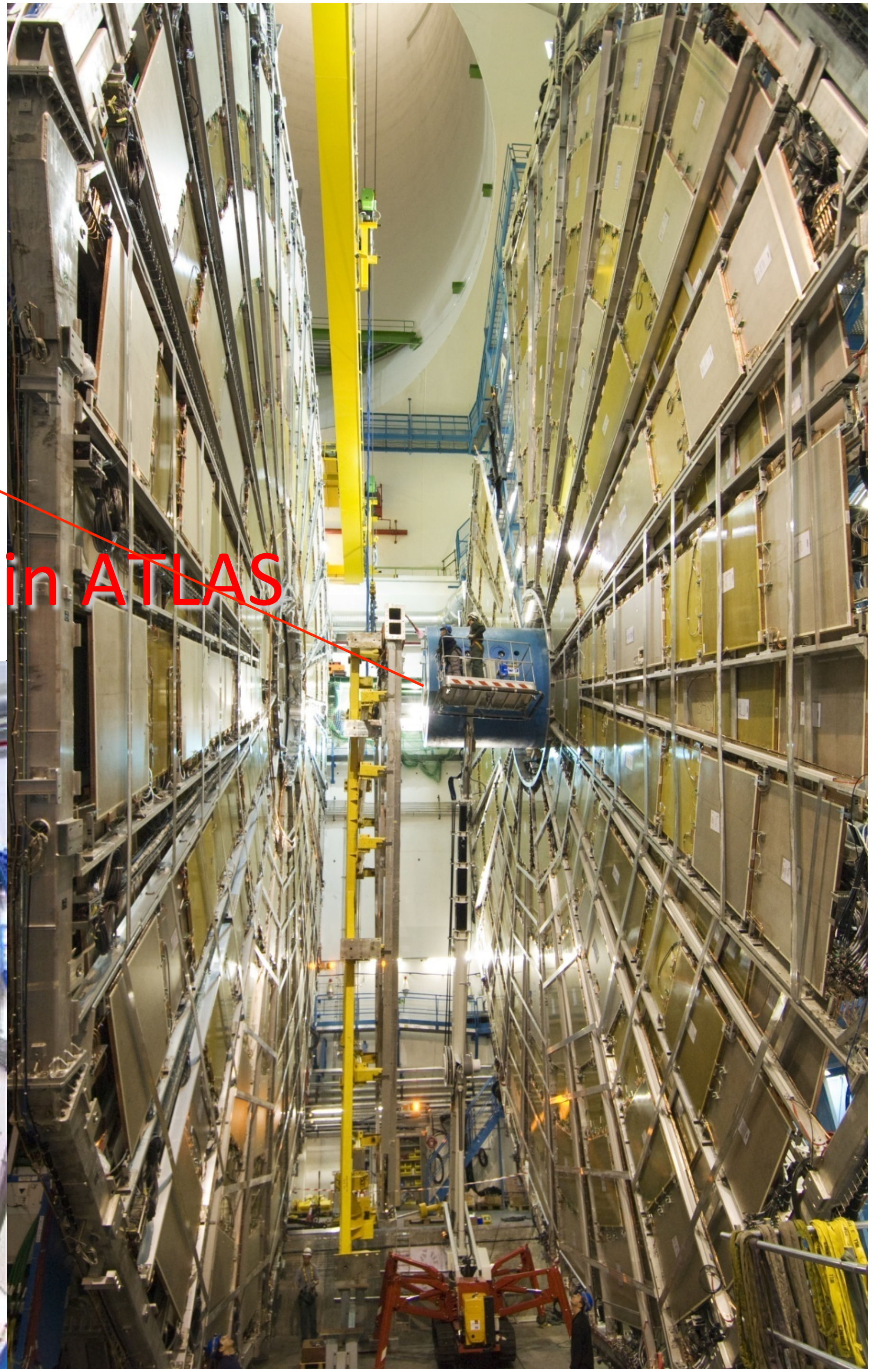

ATLAS SCT Module Designs

ATLAS Tracker Based on
Barrel and Disc Supports

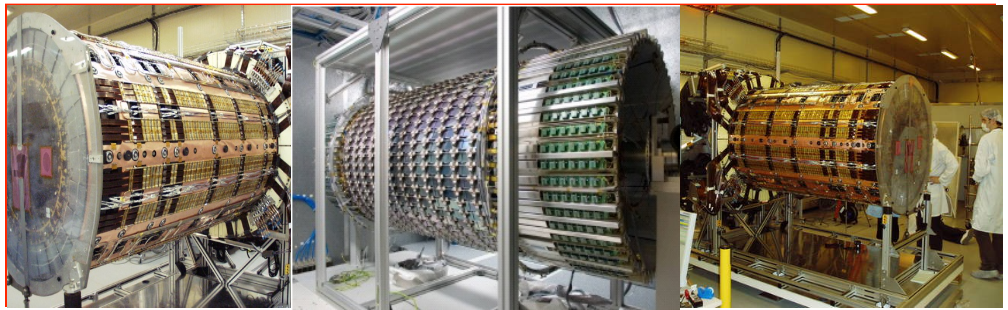

Effectively two styles of double-sided modules (2×6cm long)
each sensor ~6cm wide (768 strips of 80μm pitch per side)

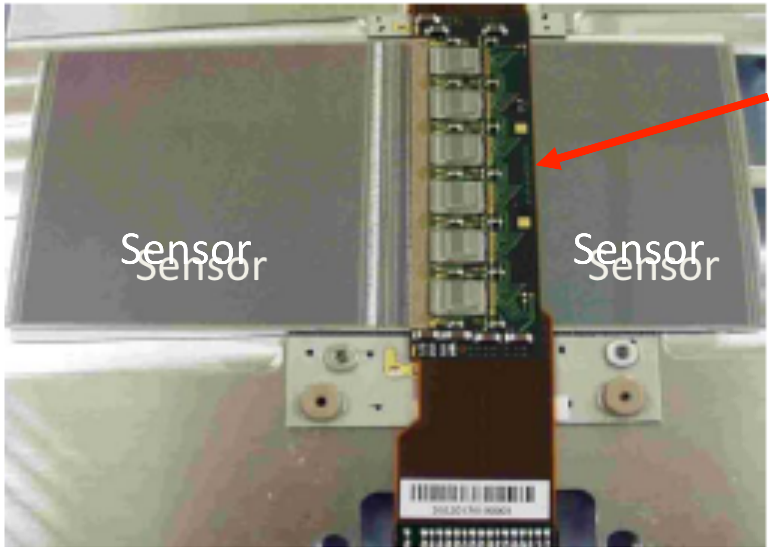

Hybrid cards carrying read-out chips and multilayer interconnect circuit

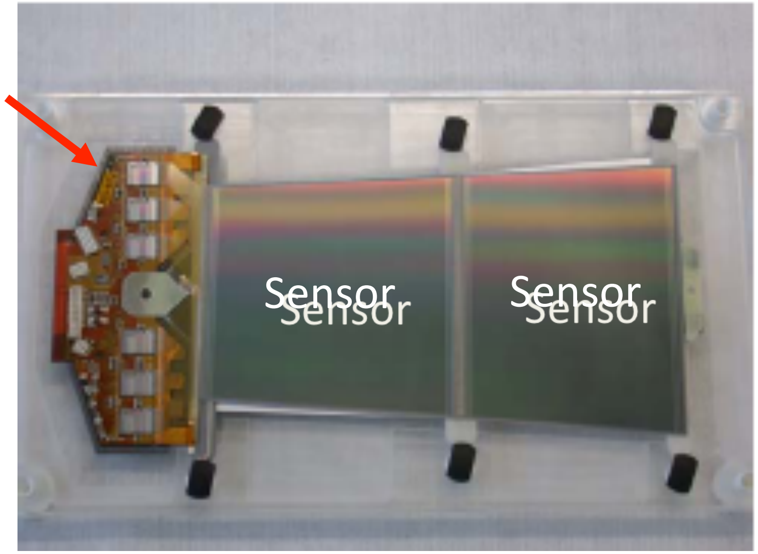

Barrel Modules
(Hybrid bridge above sensors)

Forward Modules
(Hybrid at module end)

LHC Machine Performance in 2010

"Luminosity" measured in units of b^{-1} per second (or $cm^{-2}s^{-1}$) since this multiplied by σ gives event rate
1b (barn) is $10^{-28}m^2$ or 100 fm^2
Cross-section (σ) is a measure of the probability of a process per flux of incoming particles, so if luminosity, L, represents the flux as seen be all the protons in one beam of oncoming protons in the other, this multiplied by the total cross-section, σ_{pp}, is the total event rate.
For sub-processes, the idea of a cross-section can still be used to give the event rate for that sub-process when multiplied by L
The design number of protons per bunch, 1.1 x 10^{11} , was first achieved 10th June 2010 and is now routine. The emphasis now is to increase the number of bunches circulating at any time in the LHC and then to further improve the final focus. Record luminosity: ~ 4 x 10^{31} $cm^{-2}s^{-1}$ achieved 24th September

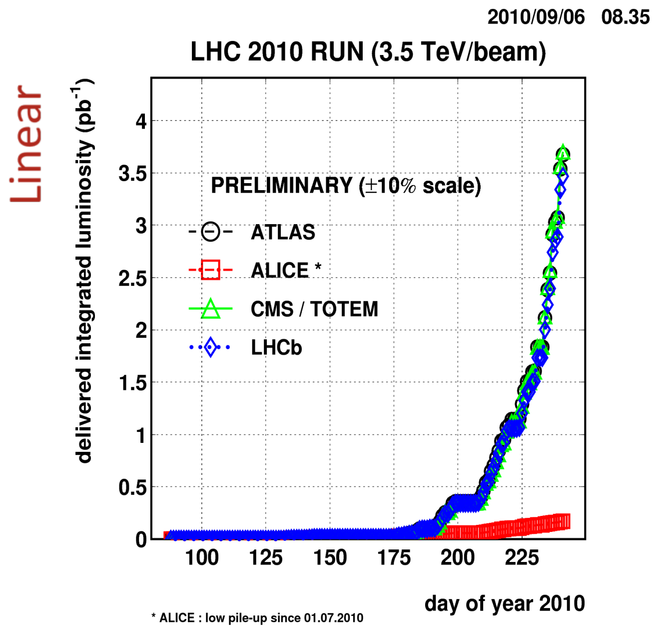

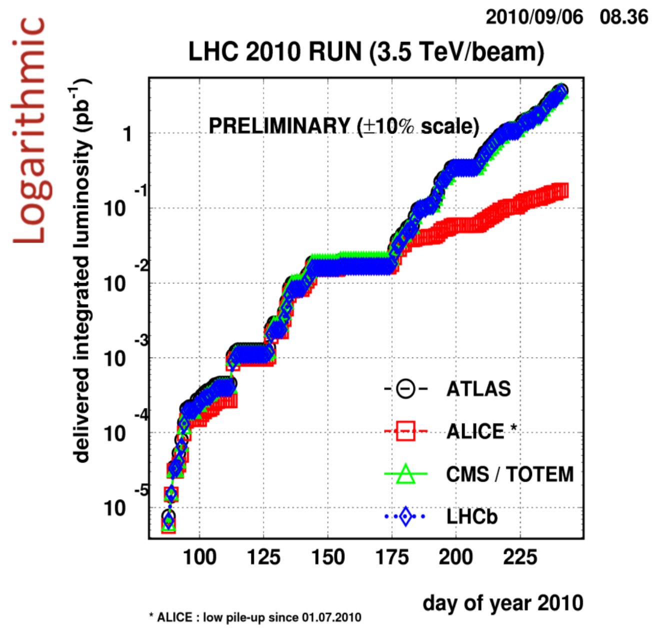

Examples of Possible ATLAS/CMS Physics Reach by Year

("Integrated Luminosity" is luminosity × time and is a measure of number of total number of eve

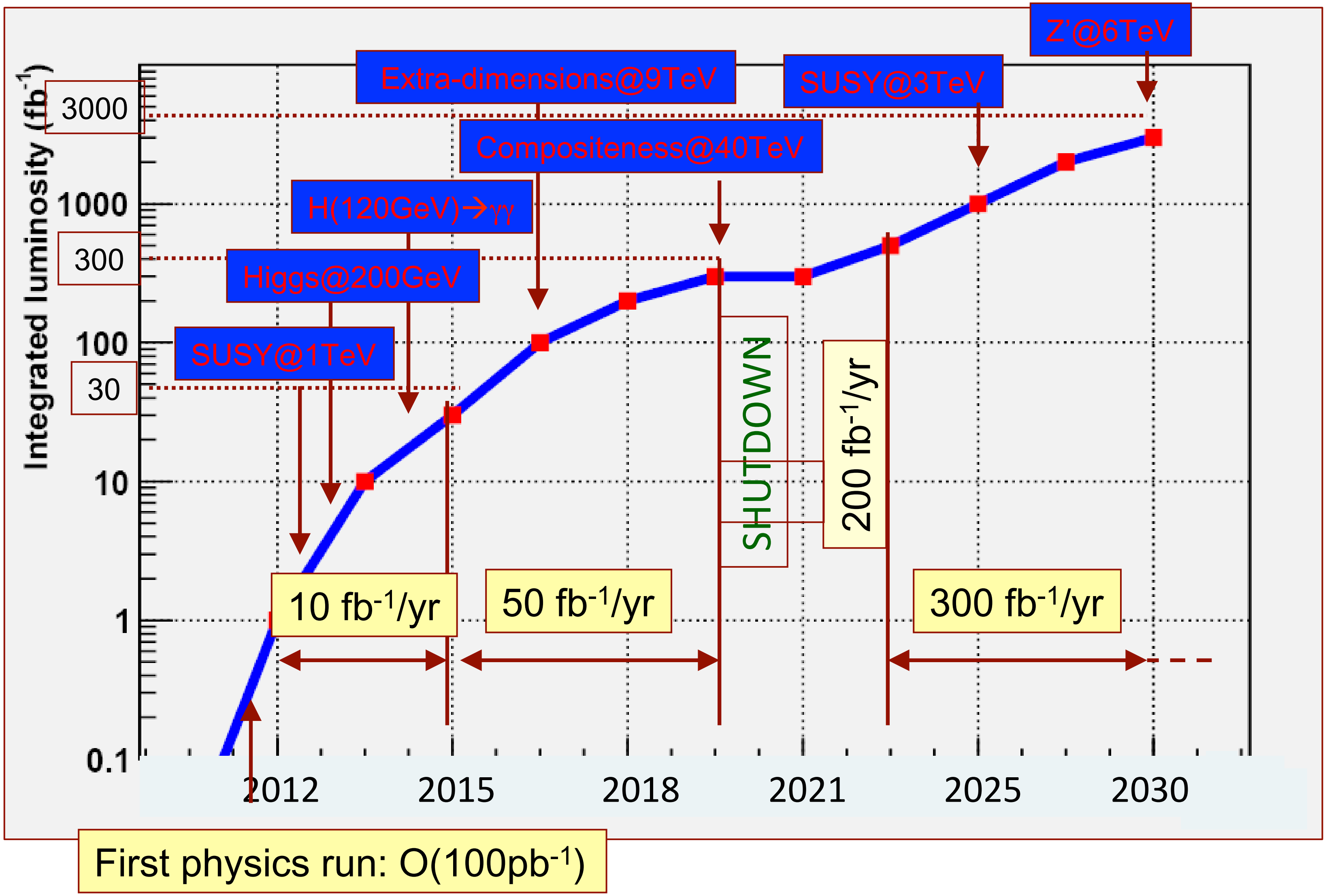

The challenge: Super LHC - visually

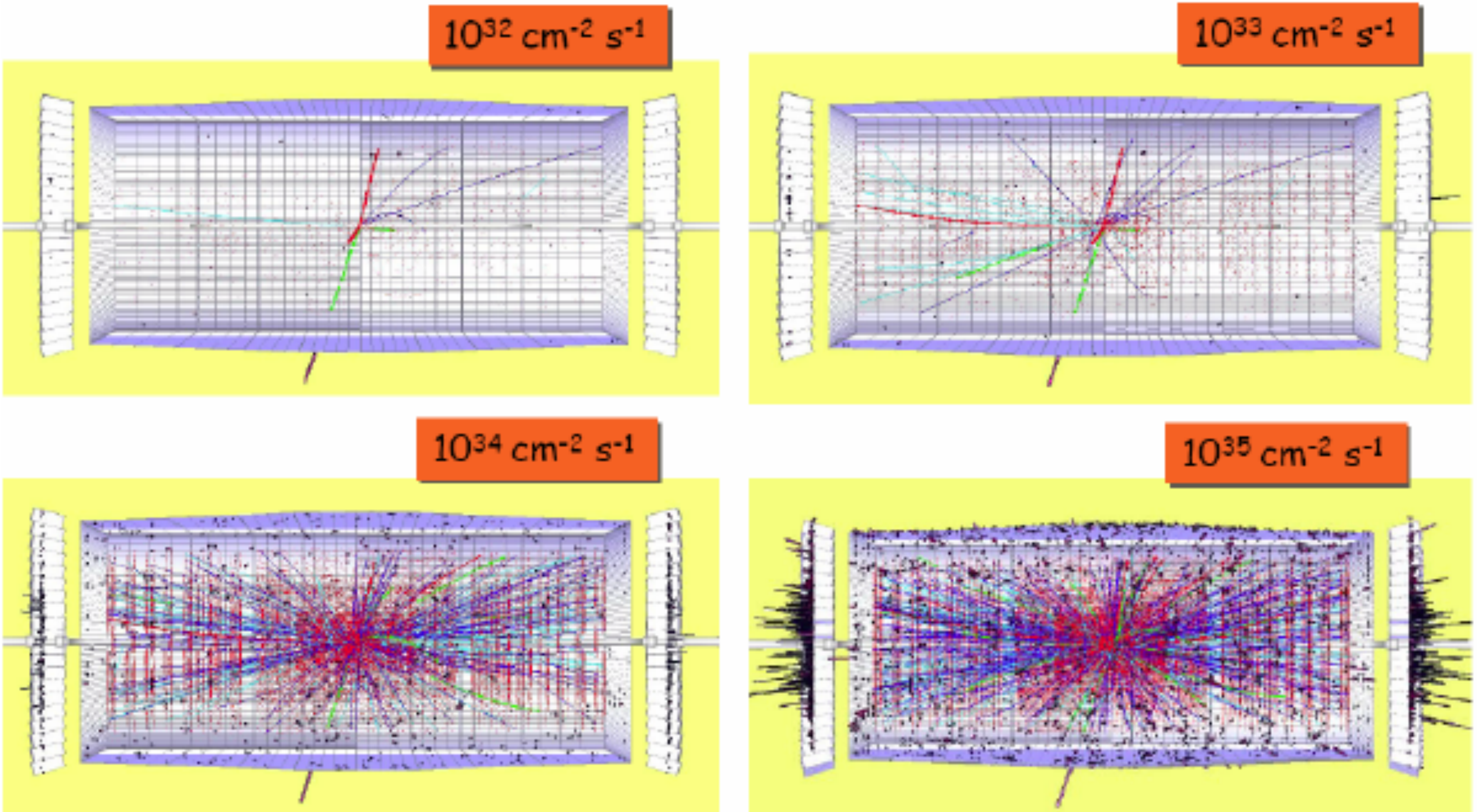

LHC luminosity **SLHC luminosity ~300-400 interactions/bx**

ATLAS All-Silicon Tracker Upgrade

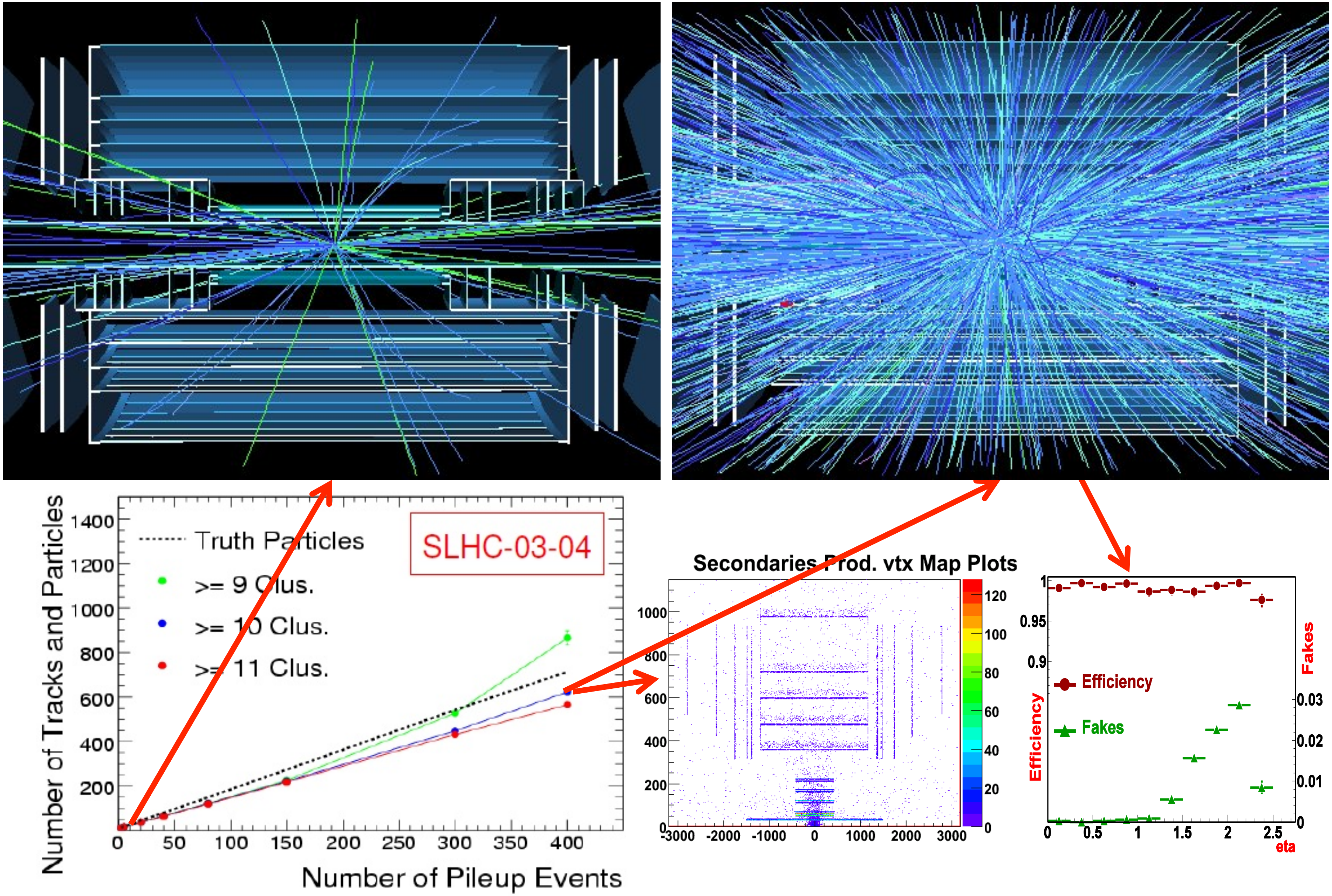

Current Silicon Microstrip (SCT) Material

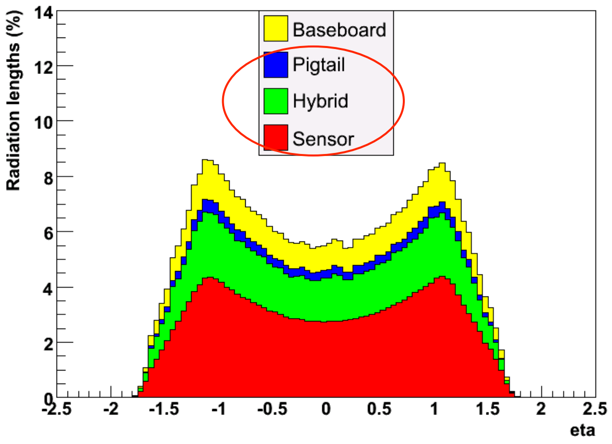

Current Silicon Tracker
(4 barrel strip layers)

Module Material

Support Material

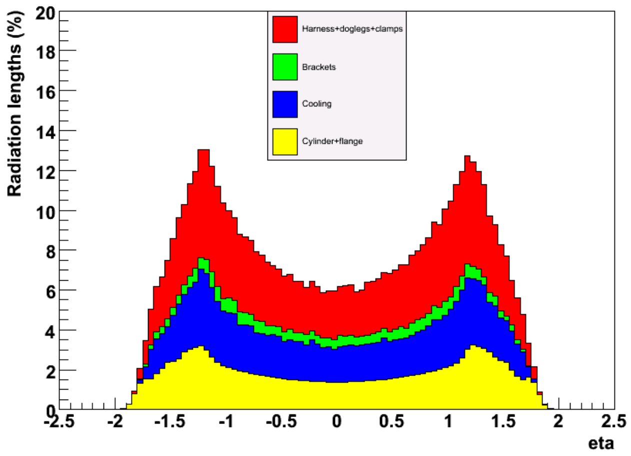

Old ATLAS Barrel Module
12 ASIC of 300μm thickness for double-sided module read-out
(*ie* just 6 read-out chips per side)

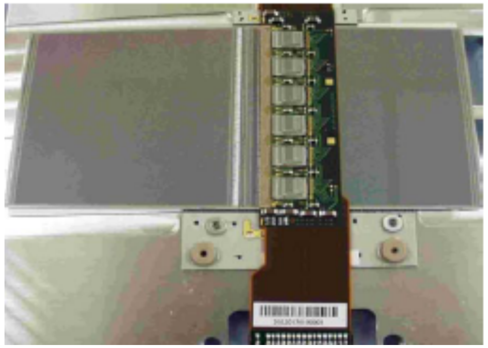

New ATLAS sLHC-Tracker Module will have 80 ASICs in two hybrid fingers for just one-sided read-out

"The barrel modules of the ATLAS semiconductor tracker". Nucl.Instrum.Meth.A568:642-671,2006.

Table 1
Radiation lengths and weights estimated for the SCT barrel module

Component	Radiation length [%Xo]	Weight [gr]	Fraction [%]
Silicon sensors and adhesives	0.612	10.9	44
Baseboard and BeO facings	0.194	6.7	27
ASIC's and adhesives	0.063	1.0	4
Cu/Polyimide/CC hybrid	0.221	4.7	19
Surface mount components	0.076	1.6	6
Total	1.17	24.9	100

Hybrid area per module roughly ×2 at sLHC - much higher R/O granularity

Stave: Hybrids glued to Sensors glued to Bus Tape glued to Cooling Substrate

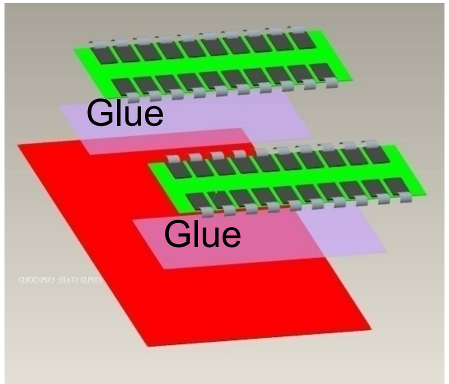

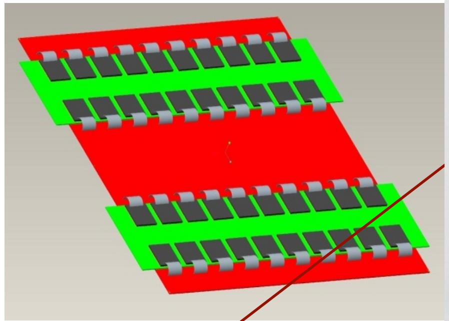

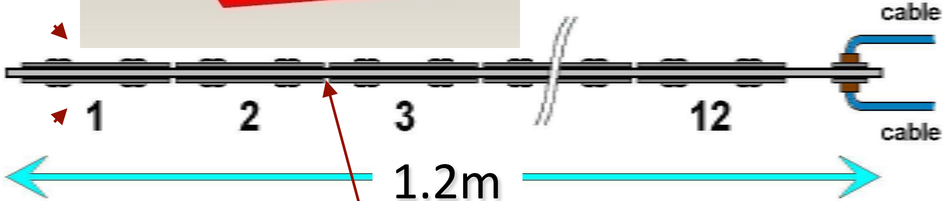

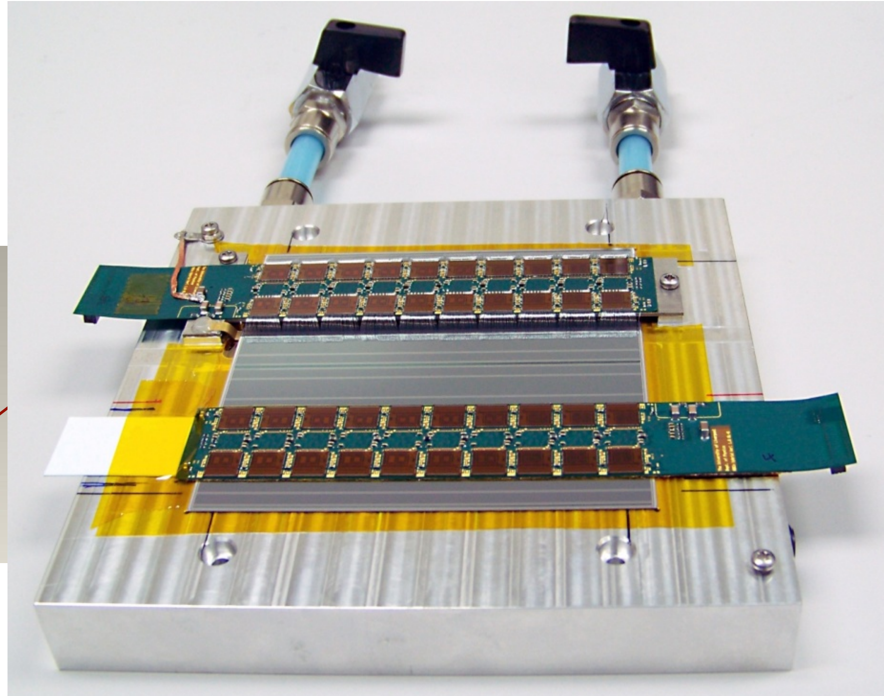

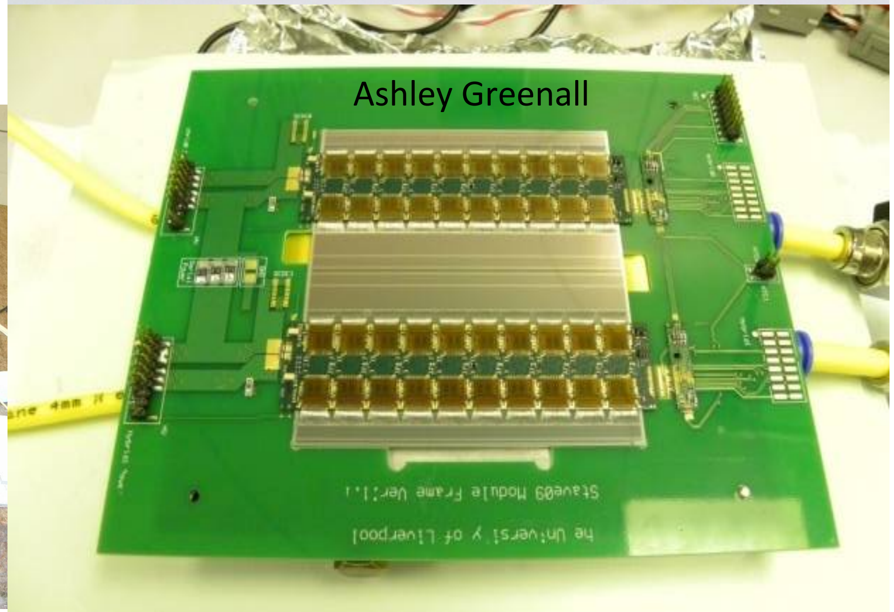

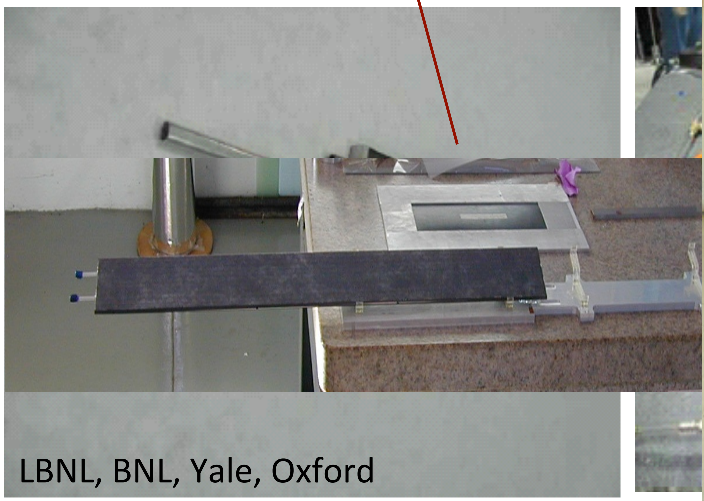

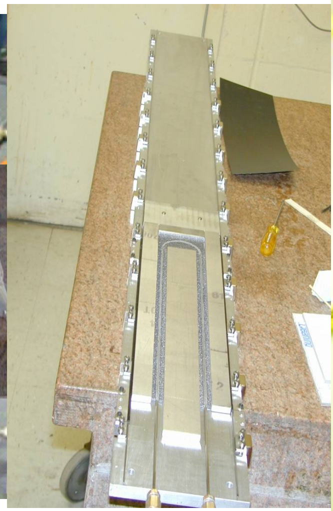

ATLAS Pixel Upgrade ASIC

- New Front-End chip (FE-I4) for smaller pixel dimensions being delivered
- Fabricated for Phase-I b-layer replacement (IBL)

→ an intermediate step towards the full upgrade.

Performance improvements for the detector (issues more related to FE chip):

- Reduce radius → Improve radiation hardness planar , 3D sensors, diamond, gas, …?)
- Reduce pixel cell size and architecture related dead time (→ deign FE using 0.13 μm 8 metal CMOS)
- increase the module live fraction → increase chip size, 19×20 mm^2

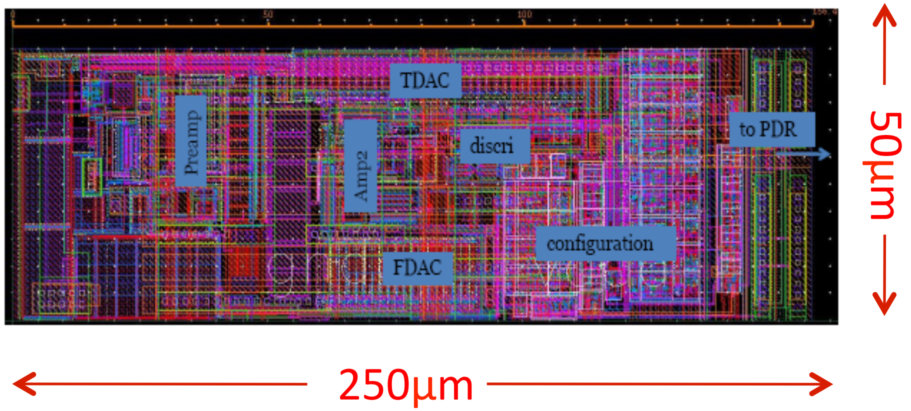

Main Parameter	Value	Unit
Pixel size	50 x 250	μm^2
Input	DC-coupled negative polarity	
Normal pixel input capacitance range	300÷500	fF
In-time threshold with 20ns gate	4000	e
Two-hit time resolution	400	ns
DC leakage current tolerance	100	nA
Single channel ENC sigma (400fF)	300	e
Tuned threshold dispersion	100	e
Analog supply current/pixel @400fF	10	μA
Radiation tolerance	200	MRad
Acquisition mode	Data driven with time stamp	
Time stamp precision	8	bits
Single chip data output rate	160	Mb/s

FE-I4 (B-layer Replacement) Specifications: main parameters

SLHC Phase-II Pixels Outer Layer Stave Concept

4 FEI-I4 ASIC module

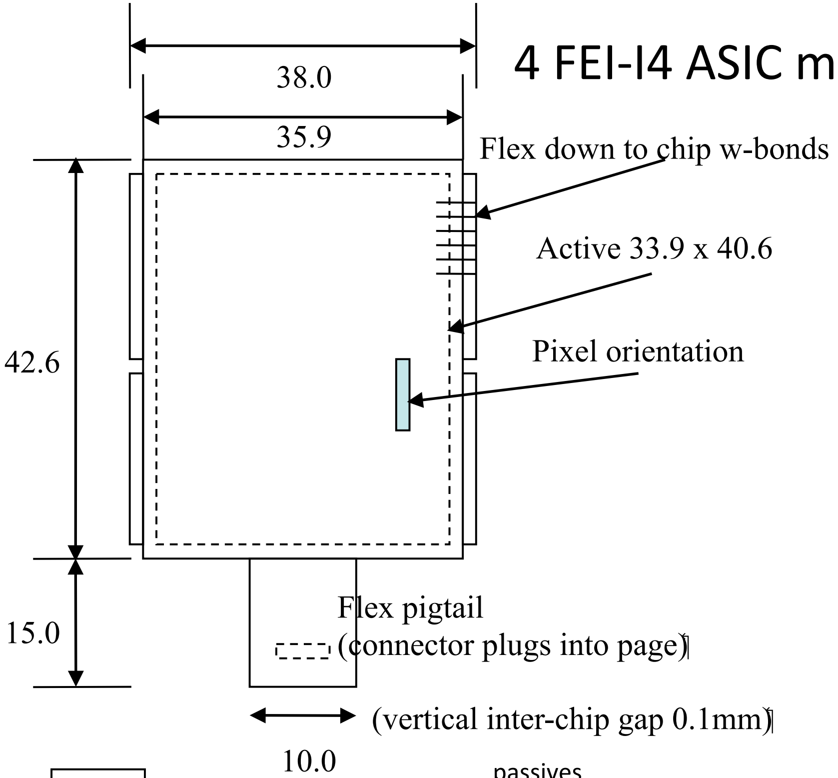

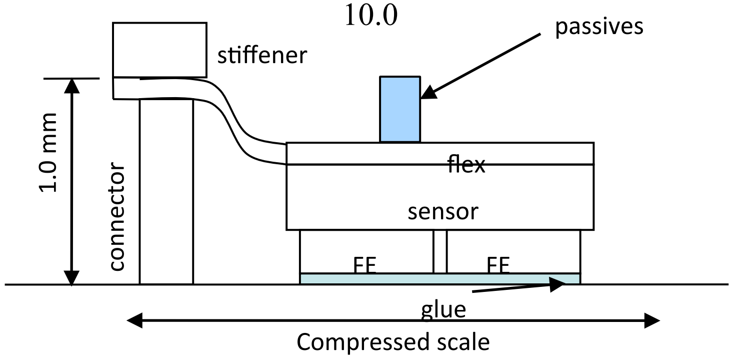

4 FEI-I4 compatible sensors from IBL project suitable for prototyping

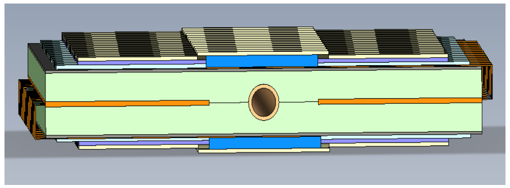

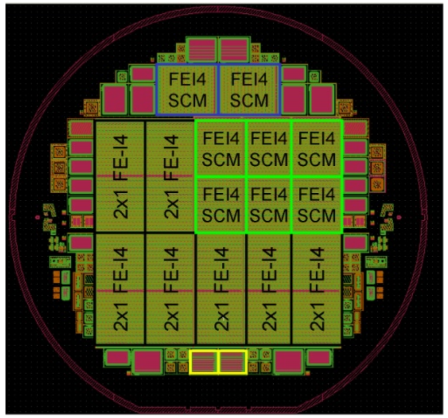

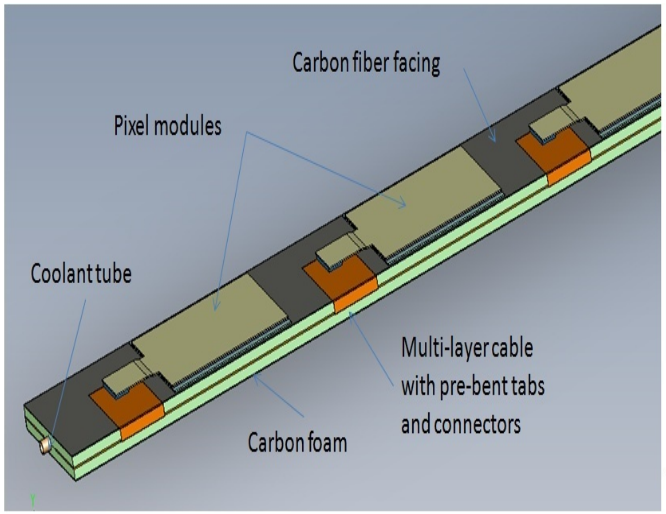

Possible Phase-II Pixel Mechanics

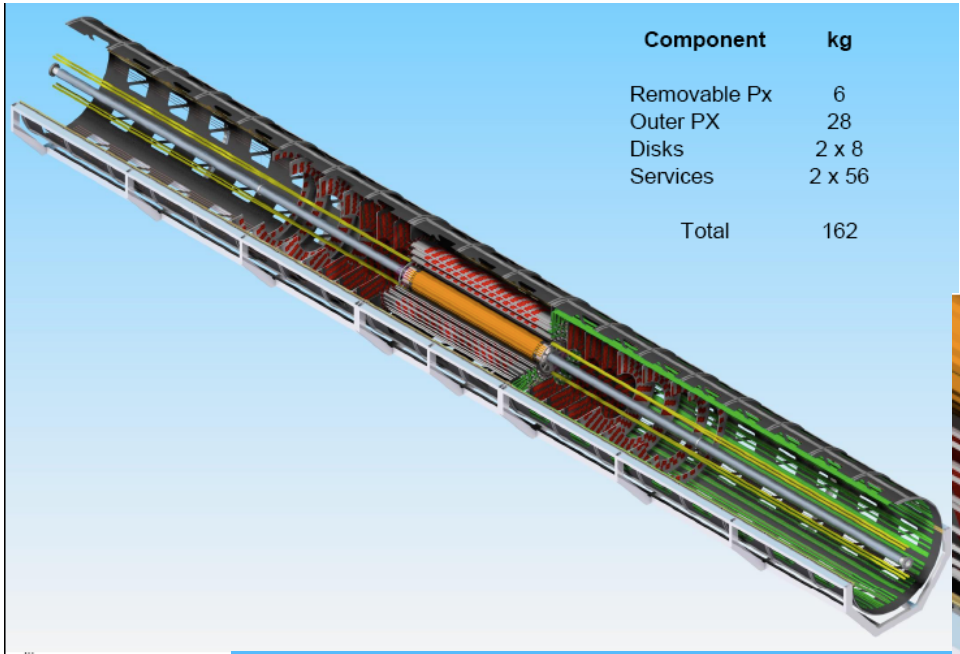

Component	kg
Removable Px	6
Outer PX	28
Disks	2 x 8
Services	2 x 56
Total	162

Independent thermal enclosure for replacement pixel package

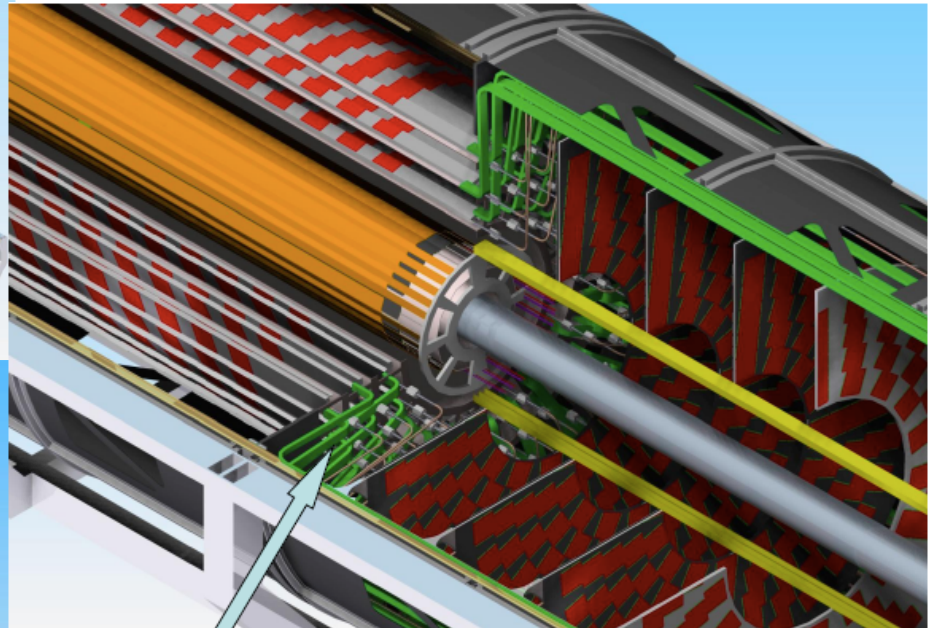

SLAC

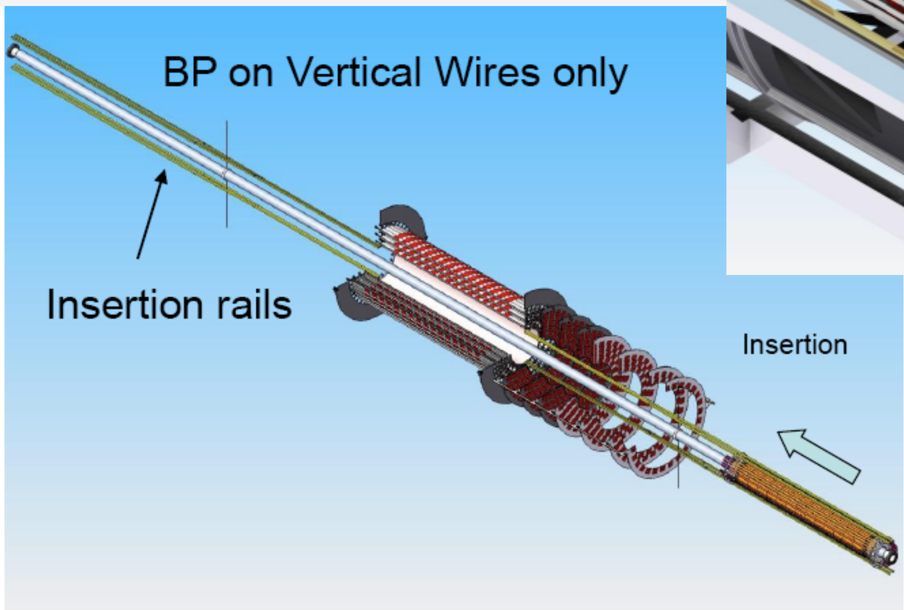

IBL remains separately insertable

Independently Installable Pixels

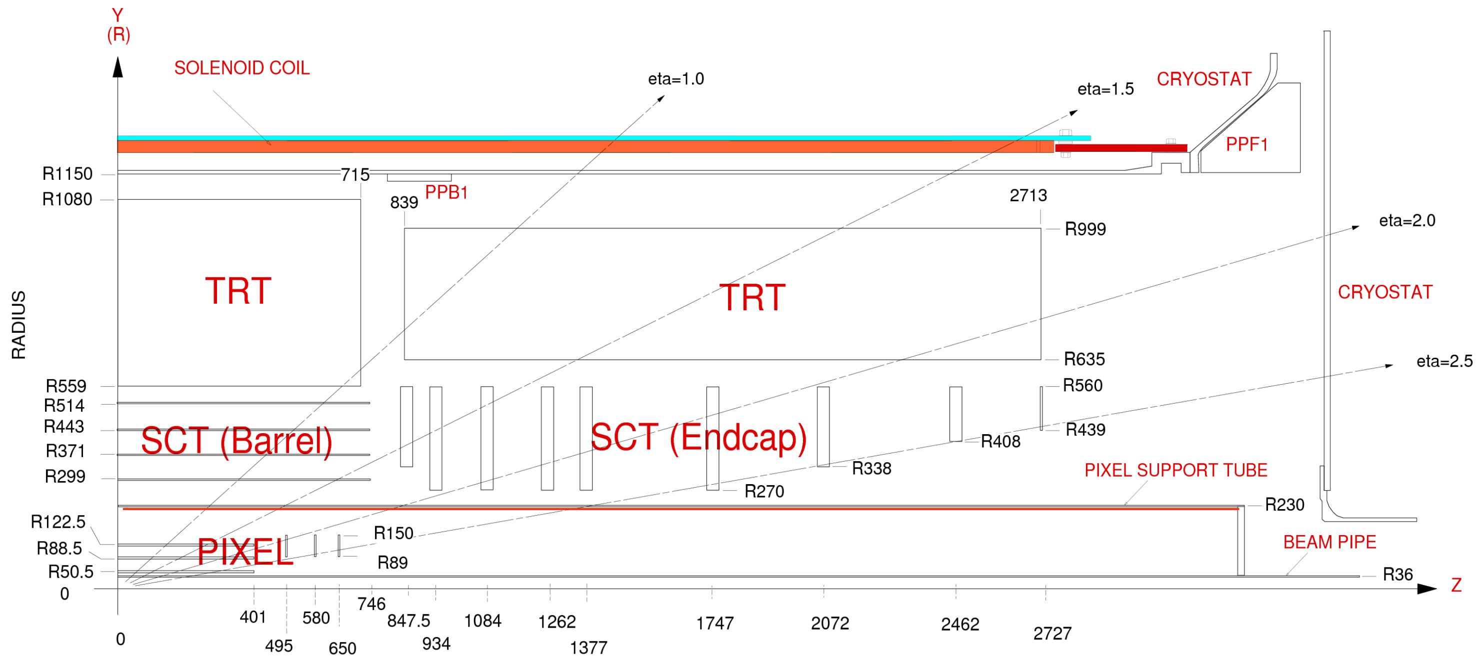

Consistent with installation within current pixel radii

Current SCT quarter section layout showing pixel support tube at 23cm radius

Proposed All-silicon tracker layout showing radius of current pixel support tube.

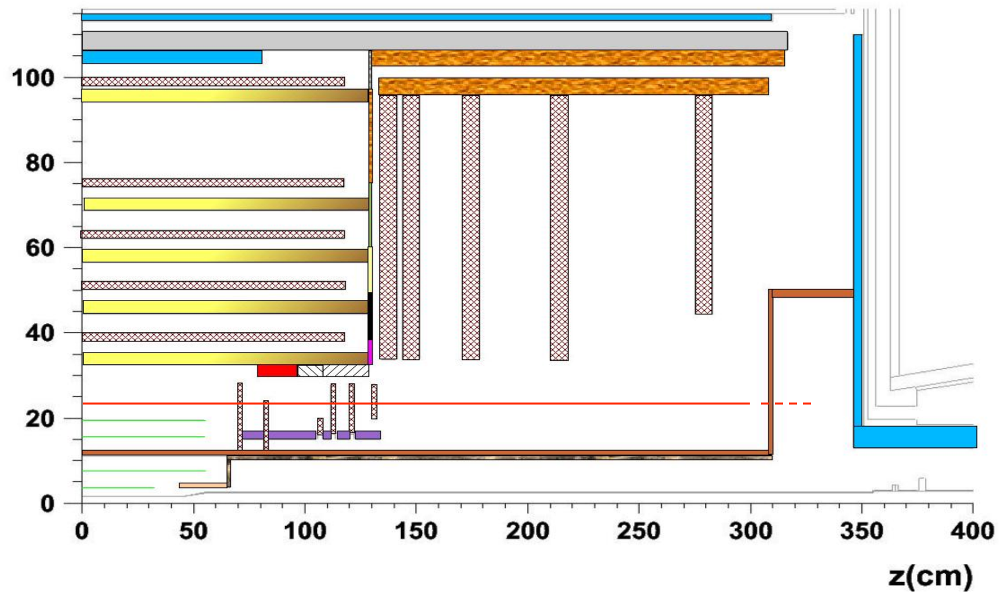

Direct Processing of Hybrid Circuit on Silicon Sensor

(Ultimate reduction in mass and assembly complexity.)

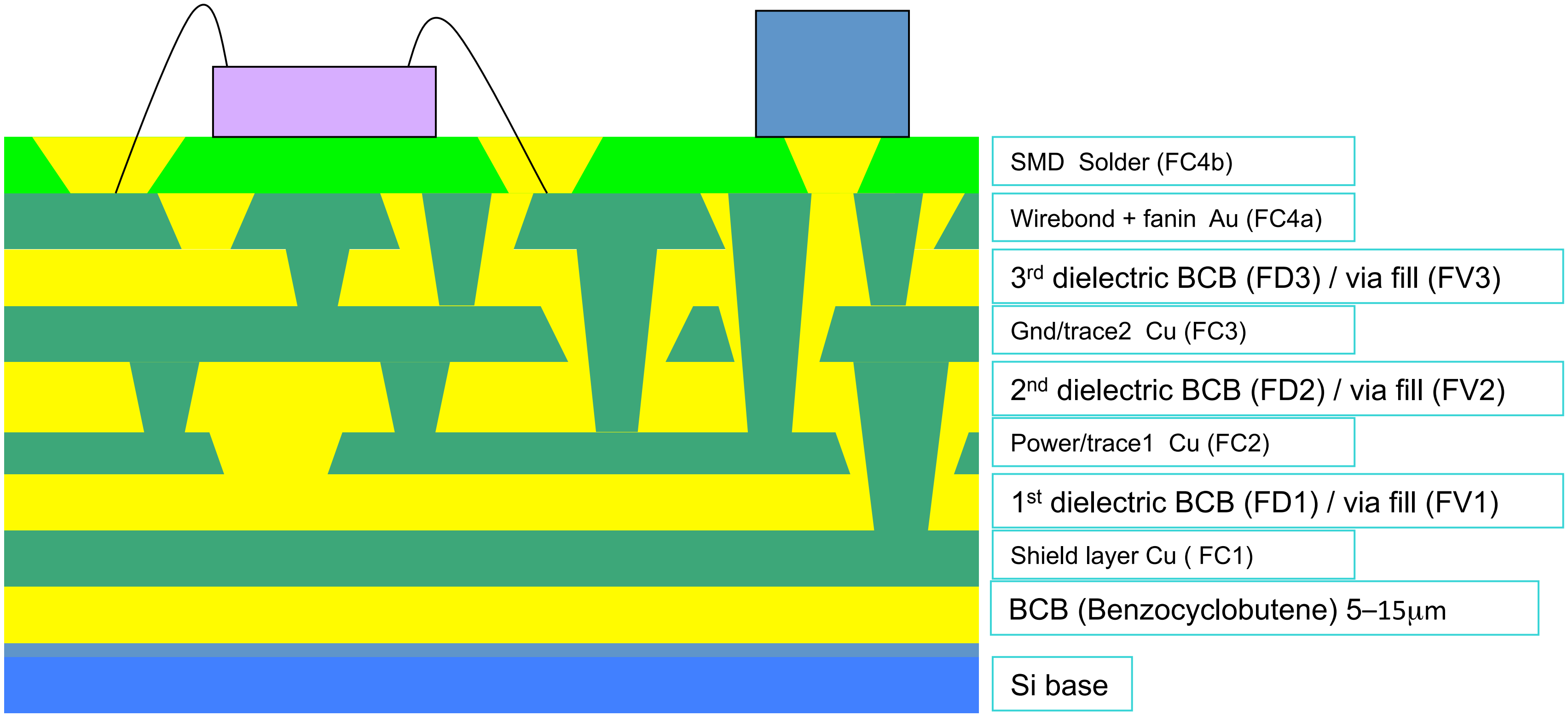

Does away with need for hybrid substrate and thick-film processing.
Prototyping for ATLAS underway with several European manufacturers.

Ultimate Interconnection: Vertical Integration

Ideal solution for reducing material and easing assembly in detector system is to integrate electronics and sensors into a single item

… if affordable

- This has been a "dream" for many years
- More complex detectors, low mass
- Liberate us from bump/wire bonding

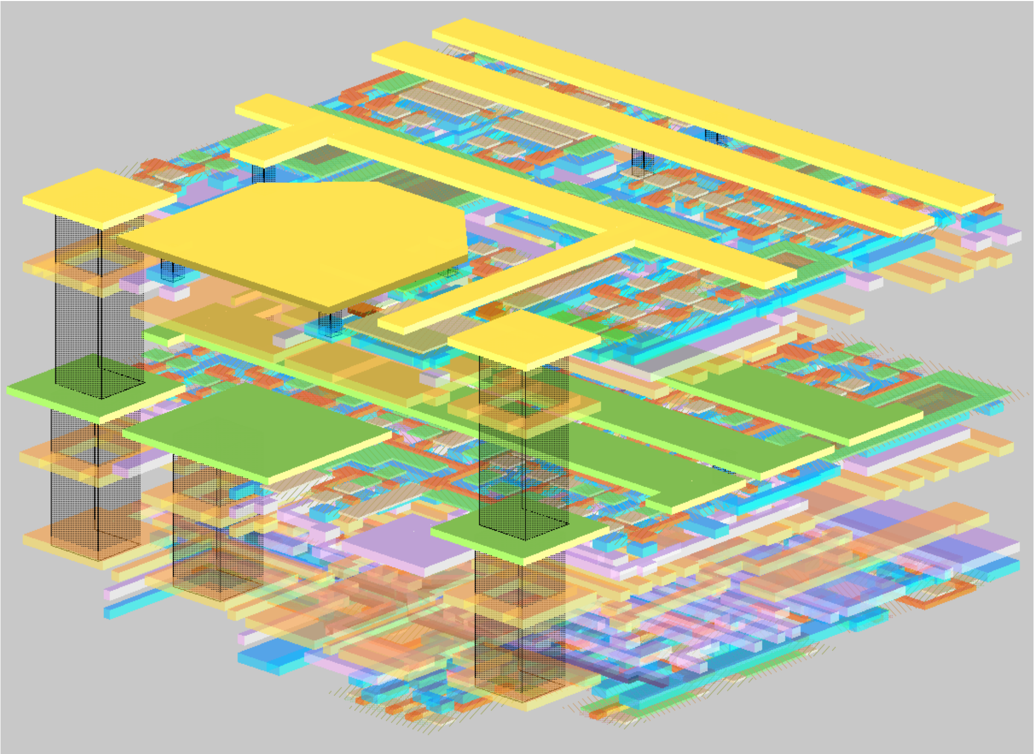

Many different aspects of these new technologies such as SLID (solid liquid inter-diffusion), TSV (through silicon vias), ICV (inter-chip vias) as well as more highly integrated concepts.

Commercial technologies becoming available for custom design:
IBM, NEC, Elpida, OKI, Tohoku, DALSA, Tezzaron, Ziptronix, Chartered, TSMC, RPI, IMEC……..

But are they all, or even, are any technologies radiation hard?

Alcuni commenti finali

- I rivelatori al silicio hanno conquistato un ruolo sempre maggiore nei grandi sistemi di tracciamento dalla loro introduzione nel 1980 circa. Nell'attuale LHC costituiscono la parte essenziale dei tracciatori e stanno funzionando egregiamente. Sono piu' di un ordine di grandezza piu' veloci e precisi rispetto agli esperimenti precedenti.
- Le previsioni per il futuro di LHC richiedono di nuovo un miglioramento di un ordine di grandezza in alcune performance dei rivelatori.
- Lo sviluppo di rivelatori tanto performanti e' in pieno corso con risultati molto incoraggianti.
- I rivelatori a semiconduttore (specialmente Silicio) stanno mostrando una adattabilita' e efficacia impressionanti e sono capaci di fronteggiare sfide di crescente difficolta' grazie ad uno sviluppo che sposta di vlta in volta i limiti della tecnologia. Sicuramente in Super LHC, ma anche nelle prossime future possibili macchine, non si ha l'impressione che questo tipo di rivelatore venga spodestato da altre tecnologie (nanostrutture .....?.....).

Bibliogaphy & credits

- S. M. Sze: Semiconductor Devices, Physics and Technology, Wiley 1985
- H. Spieler: Semiconductor Detector Systems, Oxford University Press, 2005
- Rossi, Fischer, Rohe, Wermes: Pixel Detectors: from Fundamentals to Applications, Springer 2006
- Hartmann, F: Evolution of Silicon Sensor Technology in Particle Physics, Springer 2009.

Extensive material can be found at H. Spieler site:
http://www-physics.lbl.gov/~spieler/
And here: from M. Krammer, F. Hartmann : EDIT 2011
Excellence in Detectors and Instrumentation Technologies
CERN, Geneva, Switzerland - 31 January - 10 February 2011
http://indico.cern.ch/getFile.py/access?contribId=0&resId=0&materialId=slides&confId=124392